Optimization of a T7 RNA polymerase expression system for high-yield protein production in *Cupriavidus necator* H16

Matteo Vajente[a], Hendrik Ballerstedt[b], Lars Mathias Blank[b], Sandy Schmidt[a,*]

[a] Department of Chemical and Pharmaceutical Biology, Groningen Research Institute of Pharmacy, University of Groningen, Antonius Deusinglaan 1, Groningen 9713AV, The Netherlands.

[b] Institute of Applied Microbiology (iAMB), Aachen Biology and Biotechnology (ABBt), RWTH Aachen University, Worringerweg 1, 52074 Aachen, Germany, WSS research centre “catalaix”.

*Correspondence: s.schmidt@rug.nl

Abstract

Many chemical manufacturing routes are being replaced with enzymatic processes to improve sustainability and reduce the use of harmful chemicals. Enzyme production is often the main bottleneck of the process, and proteins are frequently produced using the workhorse *E. coli* BL21(DE3) and its derivatives. However, other bacteria with beneficial characteristics can also be engineered for this purpose. *Cupriavidus necator* H16 (*C. necator*), for example, is a Gram-negative bacterium well-known for its lithoautotrophic metabolism and high polyhydroxybutyrate (PHB) accumulation. Previous studies have demonstrated high-yield protein production without inclusion body formation, which is one of the main challenges when producing enzymes in *E. coli*. Nevertheless, high-yield protein production in *C. necator* remains an understudied field. Here, we optimized a T7 RNA polymerase genetic system to improve protein production in *C. necator*. We investigated the impact of codon usage, different inducible promoters, and several genetic elements by expressing the fluorescent reporter protein GFP. Codon usage was the main factor limiting protein production in *C. necator*. Tuning the RBS strength also strongly reduced leakiness of the promoter. As an application, we compared the performance of our engineered *C. necator* T7 RNA polymerase-based system to that of an *E. coli*-based T7 system using the ene-reductase YqjM from *Bacillus subtilis*. The optimized protein expression system in *C. necator* outperformed the gold standard, *E. coli* BL21(DE3), in producing soluble, FMN-loaded enzyme. This result highlights the potential of non-model bacteria to achieve high-yield enzyme production and promote the transition to biocatalysis-driven chemical synthesis.

Keywords

Cupriavidus necator, T7 RNA polymerase, protein production, biocatalysis, metabolic engineering

Highlights

- T7 RNA polymerase-driven protein expression in the bacterium *Cupriavidus necator* (*C. necator*)
- Codon usage tuning was essential to increase protein production in *C. necator*
- RBS tuning influenced both leakiness and maximum expression
- T7 RNA polymerase activation decreased the final OD_{600} considerably
- *C. necator* produced more FMN-loaded enzyme than *E. coli* BL21(DE3)

Graphical abstract

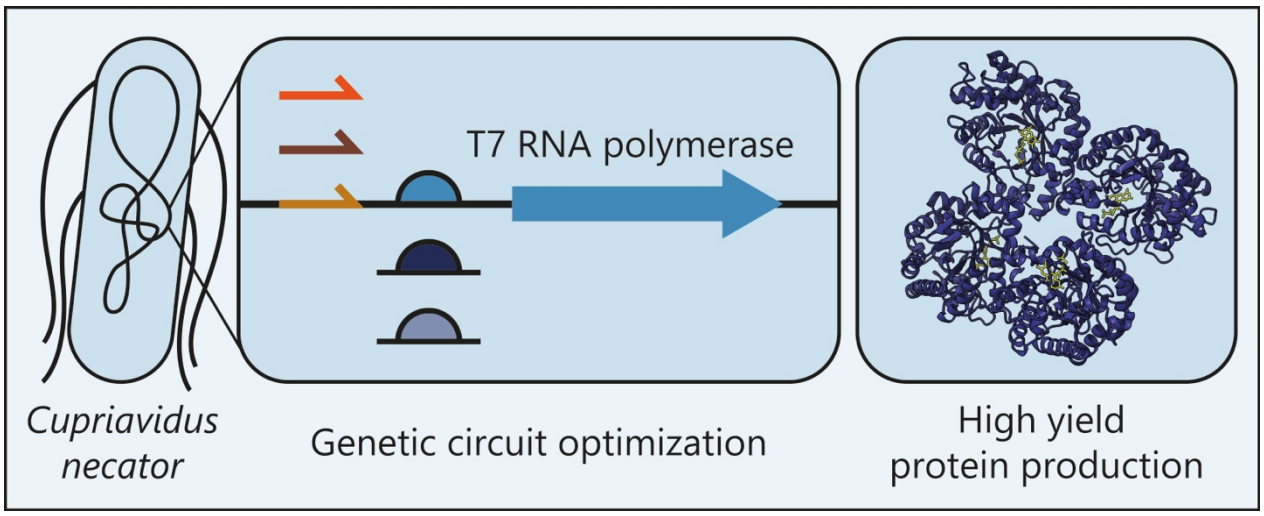

1 INTRODUCTION

Biocatalysis has emerged as a cornerstone of biotechnology, offering efficient alternatives to traditional chemical synthesis by harnessing the high selectivity and reactivity of enzymes. Central to advancing biocatalysis is the reliable and cost-effective production of enzymes, which requires not only optimization of the specific protein but also careful selection of the host system in which it is produced. Different microbial and eukaryotic hosts offer distinct advantages in terms of expression yield, post-translational modifications, scalability and economic feasibility (Tripathi and Shrivastava, 2019). Since the first application in 1986, *Escherichia coli* (*E. coli*) strains from the B lineage containing T7 RNA polymerase (T7RNAP) have become the golden standard for protein production in prokaryotic organisms (Studier and Moffatt, 1986). The T7 system allows easy induction and strong orthogonal expression of specific genes of interest. While novel *E. coli* strains have been developed to address shortcomings of the first system (e.g. leakiness) (Rosano et al., 2019), growing *E. coli* to high-cell density still suffers from various drawbacks including the formation of organic acids, proteolysis and inclusion-body formation (Choi et al., 2006; Shiloach and Fass, 2005). Moreover, several heterologous proteins such as formate dehydrogenases or hydrogenases have been troublesome to produce in *E. coli* due to a lack of appropriate chaperones or maturation factors (Ryu et al., 2024; Schiffels et al., 2013). Other non-model bacteria, such as *Cupriavidus necator* (*C. necator*, formerly known as *Ralstonia eutropha*), are currently attracting attention because of their autotrophic metabolism and potential applications in C1-based biotechnology. However, efficient protein production is still underdeveloped in such non-model strains. *C. necator* is an attractive host for protein production due to its versatile proteome (Jahn et al., 2021) and its lithoautotrophic metabolism. It is able to grow autotrophically on "Knallgas", a mixture of H_2, O_2 and CO_2, and engineered strains have shown production of various metabolites from CO_2 (Pan et al., 2021). Enzyme production has been demonstrated and quantified in both heterotrophic and autotrophic conditions, proving that protein production in autotrophic conditions is feasible (Arhar et al., 2024). In addition, the native formatotrophic metabolism of *C. necator* enables growth on formic acid, which can be synthesized from CO_2 through electroreduction (Jhong et al., 2013). Recently, formate-based production of enzymes for biocatalysis in this host has also been reported (Hallamaa et al., 2025). Therefore, *C. necator* is a suitable chassis for upgrading CO_2-rich effluents into proteins of interest for more sustainable biochemical synthesis. Food proteins are another promising market sector for hydrogen-oxidizing bacteria (Angenent et al., 2022; Bernal-Cabas et al., 2025), as *C. necator* is generally recognized as safe (GRAS). This microorganism can be grown at high cell densities in both autotrophic and heterotrophic conditions (Srinivasan et al., 2002; Tanaka et al., 1995). Its high protein content, which can account for up to 83% of cell dry weight depending on the carbon source and growth conditions (Ismail et al., 2025, 2024), emphasizes its potential for producing recombinant proteins, either as a whole-cell biocatalyst or for further protein purification. Interestingly, *C. necator* has been shown to express enzymes that *E. coli* is not able to produce or that cause the formation of inclusion bodies (Ryu et al., 2024; Srinivasan et al., 2002). Thus far, the best-performing recombinant expression method in *C. necator* used a T7RNAP-based system; however, it relied on a proprietary strain derived from H16 (Barnard et al., 2004; Byrom, 1994). A recent attempt to establish a T7-based system in *C. necator* H16 was unsuccessful, as the T7-driven system yielded the same amount of Red Fluorescent Protein (RFP) as a plasmid carrying the P_{BAD} arabinose-inducible promoter (Hu et al., 2020). An ideal production strain should exhibit strong gene expression and translation, leading to high yield of soluble, cofactor-loaded enzyme. In addition, it should also be tightly regulated to separate the biomass accumulation phase from the protein production phase. This is especially important when the

energy or carbon source is limited by process parameters, such as growth under autotrophic conditions. This separation could decrease plasmid loss during biomass accumulation, a known problem in *C. necator* (Ehsaan et al., 2021). Several engineering iterations have successfully improved these parameters for *E. coli* BL21(DE3) and derivatives, but no optimization has yet been attempted for protein production in *C. necator*. Although several studies have demonstrated its ability to synthesize small molecules from CO_2 (Pan et al., 2021), few have quantified heterologous enzyme production (Arhar et al., 2024; Assil-Companioni et al., 2019; Barnard et al., 2004; Gruber et al., 2016; Ryu et al., 2024).

In this study, we describe the establishment of an inducible T7 RNA polymerase system in *C. necator*. During several rounds of iterative engineering, we examined the impact of RBS strength and codon usage on the expression of T7RNAP and green fluorescent protein (GFP). We investigated different inducible promoters (rhamnose and salicylate) and variants of the T7 promoter. Finally, we evaluated the performance of our system by producing YqjM, a flavin-dependent ene-reductase of biocatalytic interest. This improved recombinant protein production system enables the easy expression of genes of interest and expands the array of prokaryotic chassis for protein production. This is especially true given the vast genome and availability of maturation cofactors in *C. necator*. Furthermore, its native lithoautotrophic metabolism enables enzyme production directly from CO_2 or formate, making *C. necator* a promising chassis for C1-based biocatalysis.

2 Materials and Methods

Chemicals, Bacterial Strains, and Culture Conditions

All chemicals used were purchased from Sigma−Aldrich Ltd., VWR International LLC, or Carl Roth GmbH in the highest available purity. The strains, plasmids, primers, genetic elements, and gene sequences used in this study are listed in Tables 1, S1, S3, and S6. *C. necator* and *E. coli* were grown in *lysogeny* broth (LB, 10 g/L tryptone, 10 g/L NaCl, 5 g/L yeast extract) at 30 °C (*C. necator*) and 37 °C (*E. coli*), shaking orbitally at 200 rpm. Agar agar was added to a final concentration of 2% to obtain LB agar. When appropriate, media was supplemented with antibiotics at the specified concentrations: kanamycin (*E. coli*: 50 µg/mL, *C. necator*: 200 µg/mL (routine cultivations) or 400 µg/mL (selection after electroporation)), tetracycline (*E. coli*, *C. necator*: 15 µg/mL), and gentamicin (*C. necator*: 20 µg/mL).

Table 1: Strains used and created in this study.

Strain	Genotype	Reference
Cupriavidus necator ΔRM	*C. necator* H16 ΔE6A55_RS00030 ΔE6A55_RS00035 ΔE6A55_RS00040 ΔE6A55_RS00045	(Vajente et al., 2024)
Cupriavidus necator ΔnagR	*C. necator* ΔRM Δ*nagR* (E6A55_RS01580)	This study
Cupriavidus necator T7R	*C. necator* ΔRM Δ*nagR* (E6A55_RS01580) *rhaRS,* P_{rha}-RBS_A-*T7RNAP* (not codon optimized)	This study
Cupriavidus necator T7S	*C. necator* ΔRM Δ*nagR* (E6A55_RS01580) $P_{H16\_RS08125}$-*T7RNAP* (not codon optimized)	This study
Cupriavidus necator T7R2	*C. necator* ΔRM *rhaRS,* P_{rha}-B0034m-*T7RNAP* (codon harmonized)	This study

Cupriavidus necator T7RT	*C. necator* ΔRM *rhaRS,* P_{rha}-B0034m-*T7RNAP* (codon harmonized) with SIBR insertion between G442 and L443	This study
Escherichia coli DH5α	*F- Φ80lacZΔM15 Δ(lacZYA-argF) U169 recA1 endA1 hsdR17(rk-, mk+) phoA supE44 thi-1 gyrA96 relA1 λ-*	ThermoFisher Scientific
Escherichia coli S17-1	(DSM 9079) *RP4−2(Km::Tn7,Tc::Mu-1) pro-82 recA1 endA1 thiE1 hsdR17 creC510*	DSMZ
Escherichia coli BL21(DE3)	*fhuA2 [lon] ompT gal (λ DE3) [dcm] ΔhsdS λ DE3 = λ sBamHIo ΔEcoRI-B int::(lacI::PlacUV5::T7 gene1) i21 Δnin5*	New England Biolabs

Cloning and plasmid assembly

Plasmid DNA was purified using QIAprep Spin Miniprep Kit (Qiagen). DNA purification from PCR reaction mixtures was performed using QIAquick PCR Purification Kit (Qiagen Ltd., UK). Microbial genomic DNA was extracted using the NucleoSpin Microbial DNA Kit (Macherey-Nagel). Oligonucleotide primers were synthesized by Eurofins Genomics (Ebersberg, Germany). Plasmids were sequenced by Sanger sequencing or whole plasmid nanopore sequencing (Macrogen Europe). BsaI-HFv2, BbsI-HF, and T4 DNA ligase were purchased from New England BioLabs (NEB). DpnI FastDigest was purchased from Thermo Scientific. Plasmids from the Golden Standard library were kindly provided by the authors (Blázquez et al., 2022). Plasmid pLO3 (Lenz and Friedrich, 1998) was kindly provided by Dr. Oliver Lenz (TU Berlin, Germany). A derivative plasmid without restriction patterns was used, according to a previous study (Vajente et al., 2024). Plasmid pET28a-YqjM was kindly provided by Prof. Frank Hollmann (TU Delft, The Netherlands) (Pesic et al., 2017). All genetic parts were PCR-amplified, synthesized from Twist Bioscience, or synthesized as oligonucleotides. DNA was amplified by PCR using Q5 High-Fidelity DNA Polymerase (NEB) following the manufacturer's instructions. After PCR amplification, template DNA was removed by adding 0.5 µL of DpnI to the PCR mix and incubating the mixture at 37 °C for 1 h. To anneal oligonucleotides, equimolar amounts of complementary primers (final concentration: 30 µM) were mixed in annealing buffer (10 mM Tris, 50 mM NaCl, 1 mM EDTA, pH 7.5) and incubated in a thermocycler for 2 min at 95 °C. The temperature was then decreased by 1 °C per cycle for 70 cycles (40 s each). All plasmids were assembled using Golden Gate assembly (Engler et al., 2008). Briefly, 75 ng of PCR-amplified backbone or acceptor plasmid were mixed with linear fragments in a 1:2 molar ratio, with donor plasmids in a 1:1 molar ratio, or with annealed oligonucleotides in a 1:10 molar ratio. Golden Gate reactions were carried out in a total volume of 10 µL by mixing the DNA, ultrapure water, T4 DNA ligase buffer, T4 DNA ligase (200 U), and BsaI-HFv2 or BbsI-HF (6 U). The mixture was then incubated in a thermocycler using the following program: (37 °C, 5 min → 16 °C, 5 min) × 15-30 cycles → 60 °C, 5 min. Finally, the assembled plasmids were used to transform competent *E. coli* DH5α cells. In Tables S2-S3 the DNA fragments used to assemble each plasmid are described in detail. Plasmid maps are included in the Supplementary Information as GenBank files.

Codon usage and Codon Adaptation Index analysis

T7RNAP and YqjM were codon harmonized for *C. necator* using a previously reported codon-harmonization tool (https://codonharmonizer.systemsbiology.nl/) (Claassens et al., 2017). Codon usage tables were calculated from the coding sequences of the genomes on the Galaxy web platform, using cusp (EMBOSS) on the public server at usegalaxy.eu (Rice et al., 2000; The Galaxy Community et al., 2024). Accession numbers of the genomes used for calculations are reported in the Supplementary Information

(Table S4). Codon Adaptation Index (CAI) values were calculated using cai custom (EMBOSS) on usegalaxy.eu. Nucleic sequences and CAI values for all genes used in this manuscript are available in the Supplementary Information (Tables S3, S5). *GFPmut3* was codon optimized (the genome of the original organism was unavailable at the time) using the codon-optimization tool from Geneious Prime (Dotmatics) and the *C. necator* codon usage table calculated as described above.

E. coli Transformation

For *E. coli* transformations, 50 µL of chemically competent cells prepared following a previously published method (Inoue et al., 1990) were mixed with plasmid DNA, incubated on ice for 30 min, followed by a heat shock at 42 °C for 45 s and a subsequent incubation on ice for 2 min. Cells were recovered in 950 µL of Super Optimal broth with Catabolite repression (SOC) medium at 37 °C for 1 h, plated on LB agar with the appropriate antibiotic, and incubated overnight at 37 °C.

C. necator Electroporation

Electroporation of *C. necator* was performed as previously described (Vajente et al., 2024). Briefly, *C. necator* was streaked onto a LB agar plate and grown at 30 °C for 40 h. A single colony was then cultivated in SOB supplemented with 20 µg/mL gentamicin for 16 h at 30 °C. Fresh SOB supplemented with gentamicin was inoculated with the preculture at an initial OD_{600} of 0.1 and cultivated at 30 °C. When the cells reached an OD_{600} of 0.6, they were transferred onto ice and chilled for 5−10 min. The cells were then transferred to 50 mL tubes and centrifuged at 6000 x *g* at 4 °C for 2 min. The supernatant was removed, and the cells were resuspended in 25 mL of 50 mM $CaCl_2$ by briefly vortexing. They were then incubated on ice for 15 min. The cells were then centrifuged at 6500 x *g* at 4 °C for 2 min, and the supernatant was removed. Cells were washed twice using 25 and 15 mL of ice-cold 0.2 M sucrose, respectively. At the end of each wash, cells were centrifuged at 6500 x *g* at 4 °C for 2−3 min, and the supernatant was decanted. The cell pellet was finally resuspended in 1/100 of the initial volume (e.g., 100 mL initial cell culture to 1 mL final resuspension volume). Aliquots of competent cells were transferred into microcentrifuge tubes, frozen in liquid nitrogen and stored at −80 °C until further use. For electroporation, each aliquot was thawed on ice for 20 min, transferred into a pre-chilled 1 mm electroporation cuvette, mixed with 50−200 ng of plasmid DNA and electroporated (25 µF, 200 Ω, 1.15 kV). Super Optimal Broth (950 µL; 20 g/L tryptone, 5 g/L yeast extract, 0.5 g/L NaCl, 2.5 mM KCl, 20 mM $MgSO_4$, pH 7) supplemented with fructose (20 mM) was immediately added and the cells were transferred to a 2 mL centrifuge tube for outgrowth at 30 °C for 2 h. After the outgrowth, cells were diluted and plated on appropriate selective media.

Genome editing

Knock-in and knock-out plasmids were used for *C. necator* H16 genome modification by double homologous recombination, as explained previously (Vajente et al., 2024). Most plasmids were introduced by electroporation following the method described above. Colonies that underwent the first recombination were selected on LB supplemented with 15 µg/mL tetracycline. Positive colonies were picked and grown overnight in 5 mL of low-salt LB (LSLB) without any supplementation (10 g/L tryptone, 5 g/L NaCl, 5 g/L yeast extract). Different dilutions were plated on LSLB-agar supplemented with 180 g/L sucrose to select for *sacB*-negative colonies. When selecting for *ΔnagR* strains (*C. necator ΔnagR*, T7R, T7S), different dilutions were plated on minimum media supplemented with glucose. Colony PCR was performed to screen for double-crossover insertion and deletion mutants. Genomic DNA was extracted from the promising clones to PCR-amplify the targeted region and confirm insertion or deletion by

amplicon sequencing. All plasmids were successfully introduced by electroporation (pLONagR, pLOT7R, pLOT7S, pLOT7R2) apart from pLOT7RT. In that case, the strain *E. coli* S17-1 was used for conjugation. Briefly, *E. coli* S17-1 was transformed with plasmid pLOT7RT as explained above. The donor and acceptor strains were grown overnight in LB supplemented with the appropriate antibiotics. Then, 200 µL of each saturated solution were centrifuged and washed with LSLB before resuspension in 100 µL LSLB. The cultures were mixed and plated on LSLB without antibiotics and incubated overnight at 30 °C. The biomass was then scraped from the plate, resuspended in LB and plated on LB agar supplemented with 15 µg/mL tetracycline and 20 µg/mL gentamicin, then grown for 2 days at 30 °C. Then, positive colonies were picked, grown overnight, and tested as above.

Fluorescence Measurement

Precultures were cultivated overnight at 30 °C at 200 rpm in 96-deep well plate wells (Greiner, Masterblock, 96 well, 2 mL, PP, V-bottom) containing 0.5 mL of LB supplemented with 200 µg/mL kanamycin when necessary. The deep well plates were sealed using a gas-permeable membrane (Diversified Biotech, Breathe-Easy). The following day, the OD_{600} was measured using a spectrophotometer (biochrom, Ultrospec 10). The cultures were then centrifuged (3400 x *g*, 30 min, 4 °C), and each culture was resuspended to OD_{600} 2 using fresh medium. A new 96-deep well plate was prepared with 0.45 mL in each well. Then, each well was inoculated to an initial OD_{600} 0.2 by adding 50 µL of pre-culture. The plate was then sealed with a permeable membrane and grown at 30 °C, 200 rpm for 3 h. Each culture was then induced adding sterile solutions of L-rhamnose, sodium salicylate, or theophylline. To measure uninduced expression, some cultures were left uninduced. The deep well plate was then incubated at 30 °C, 200 rpm for 22 h. Appropriate dilutions were transferred to a 96-well black walled plate (Greiner, 96 well, PS, F-bottom µCLEAR®). Fluorescence of GFPmut3 was measured from the top at an excitation wavelength of 485 nm and an emission wavelength of 535 nm with a gain of 80 in a BioTek Synergy H1 plate reader. Biomass was determined at 600 nm as scattered light. Each value was blanked using empty media (with or without kanamycin). To determine specific fluorescence, fluorescence intensity was divided by scattered light. To normalize our results, fluorescein sodium salt was used to create a calibration curve. To measure *GFP* expression driven by constitutive promoters, the same protocol was followed without the induction step. Two-sample t test was used when comparing two samples. When comparing multiple conditions, one-way ANOVA and Tukey's multiple comparison test were used. * = adjusted p-value <0.05; ** = adjusted p-value <0.01; *** = adjusted p-value <0.001; **** = adjusted p-value <0.0001. In Figure 2, the results of the statistical analysis are reported in compact letter display: results have statistically different means (adjusted p-value <0.05) if they do not share any letter.

YqjM expression in *C. necator*

Pre-cultures were cultivated overnight at 30 °C, 200 rpm in 50 mL tubes containing 5 mL of LB supplemented with 200 µg/mL kanamycin. LB without antibiotics was used to cultivate the wild type control strains. The following day, 250 mL non-baffled Erlenmeyer flasks were filled with 50 mL of media. The pre-cultures OD_{600} was measured, and the flasks were inoculated at an initial OD_{600} = 0.1. The cultures were grown at 30 °C, 200 rpm until they reached the induction OD_{600} (0.4, 0.8, 1.2). Then, they were induced by adding rhamnose (final concentration: 10 mM). Depending on the experiment, FMN (riboflavin 5'-monophosphate sodium salt hydrate, 73-79%, fluorimetric, Sigma) was added to a final concentration of 1 µM. The cultures were then grown at the chosen temperature (22 °C, 26 °C, 30 °C) for 22 h. The final OD_{600} was measured, then the cultures were centrifuged (3400 x *g*, 30 min, 4 °C), and the wet pellet was

weighted. Cell pellets were stored at -20 °C until further analysis. Cell pellets were thawed on ice and resuspended in lysis buffer (20 mM Tris, 150 mM NaCl, pH 7.5, lysozyme), depending on the wet pellet weight (20 mL/g wet pellet). The resuspended cultures were incubated on ice for 20 min, then lysed by sonication (Branson Sonifier 450, intensity 8, duty cycle 40%, 4 cycles of 30 s sonication followed by 1 min on ice). The lysate was then centrifuged (1:15 h, 18 500 x *g*, 4 °C) to obtain the soluble extract.

YqjM expression in *E. coli* BL21(DE3)

Pre-cultures were cultivated overnight at 37 °C at 200 rpm in 50 mL tubes containing 5 mL of LB supplemented with 50 µg/mL kanamycin. LB without antibiotics was used to cultivate the control strain. The following day, 250 mL non-baffled Erlenmeyer flasks were filled with 50 mL of LB supplemented with 50 µg/mL kanamycin. Then, the flasks were inoculated at an initial OD_{600} = 0.1. The cultures were grown at 37 °C and 200 rpm until they reached OD_{600} = 0.6. Then, they were induced by adding IPTG (final concentration 1 mM). The cultures were then grown at 20°C for 20 h. The final OD_{600} was measured, then the cultures were centrifuged (3400 x *g*, 30 min, 4 °C), and the wet pellet weight was measured. Cell pellets were stored at -20 °C until further analysis. Cell pellets were thawed on ice and resuspended in lysis buffer (20 mM Tris, 150 mM NaCl, pH 7.5, lysozyme), depending on the wet pellet weight (20 mL/g wet pellet). The resuspended cultures were incubated on ice for 20 min, then lysed by sonication (Branson Sonifier 450, intensity 8, duty cycle 40%, 4 cycles of 30 s sonication followed by 1 min on ice). The lysate was then centrifuged for 1:15 h (18 500 x *g*, 4 °C) to obtain the soluble extract.

FMN determination

The fresh soluble extract samples were used to determine FMN concentration by measuring the absorbance at 452 nm using a spectrophotometer (Jasco V-650, quartz cuvette). To compare the samples, the values were normalized. For each sample, the absorbance volume was multiplied by the lysis buffer amount (to obtain the total FMN produced in the whole culture), then divided by the final OD (to obtain the specific FMN produced per OD unit). Soluble extracts from wild-type strains without YqjM expression were used as blank. A calibration curve using FMN (riboflavin 5'-monophosphate sodium salt hydrate, 73-79%, fluorimetric, Sigma) was used to convert absorbance to FMN concentration values. In order to convert FMN concentration to predicted yield, we counted each molecule of FMN as a single protein molecule.

SDS-PAGE analysis

Each fresh soluble fraction sample was analysed using sodium dodecyl sulfate-polyacrylamide gel electrophoresis (SDS-PAGE). Samples were prepared by mixing Laemmli Sample Buffer (Bio-rad) and incubating at 95 °C for 10 min. Each sample was added to a pre-cast SDS-PAGE gel (Invitrogen, NuPage, 4-12% Bis-Tris, 10 wells). PageRuler (PageRuler™ Prestained Protein Ladder, 10 to 180 kDa, Thermo Scientific™) was used as a protein ladder. The gels were run in fresh MOPS buffer (Invitrogen, NuPAGE MOPS SDS Running Buffer 20x) for 15 min at 50 V, then for 1:10 h at 150 V. The SDS-PAGE gels were stained using Rapid Protein Stain Coomassie Blue (Westburg Life Sciences) and imaged using a ChemiDoc Imaging System (Bio-Rad). To compare the amount of YqjM produced by *C. necator* in each culture condition, the Analyze/Gel tool from Fiji was used to perform gel-based quantification. To minimize the influence of loading variability in the analysis, the intensity of the YqjM band (approximately 40 kDa) was normalized using the intensity of another reference protein band (Figure S5).

3 RESULTS

3.1 T7 RNA POLYMERASE IS EXPRESSED IN CUPRIAVIDUS NECATOR H16 UNDER THE CONTROL OF TWO INDUCIBLE PROMOTERS

T7RNAP was integrated into the genome and expressed in *C. necator* under the control of two inducible promoters, activated by rhamnose and salicylate, respectively. The rhamnose inducible promoter was selected due to its tightness and its orthogonal nature in *C. necator* (Alagesan et al., 2018; Sydow et al., 2017) (yielding strain *C. necator* T7R, Figures 1A, S1). The native salicylate promoter was selected due to its tightness and high dynamic range (Hanko et al., 2020) (*C. necator* T7S, Figures 1A, S1). We speculated that using a native inducible system could lead to tighter regulation due to the optimized titration of the activator protein (NahR). We decided to integrate the two systems into the *nagR* locus, while deleting the *nagR* gene. This deletion has previously been shown to allow glucose utilization by *C. necator*, which might be advantageous when using mixed carbon sources or second-generation biomasses (Orita et al., 2012). We used this glucose-growing phenotype as a selection method for successful deletion-integration. *C. necator ΔnagR* was created and used as a negative control. After integration of the two constructs, GFPmut3 (GFP) fluorescence was used to determine protein expression level. The expression of the *GFPmut3* gene was driven by a plasmid under the control of a T7 consensus promoter and RBS B0034m, previously investigated in *C. necator* (Keating and Young, 2023). We used our recently developed plasmid system (pMVRha) as a benchmark (Vajente et al., 2024) (Figure 1A). *GFP* was successfully expressed in both T7 strains using multiple concentrations of rhamnose and salicylate (Figure 1B). The strain *C. necator* T7S exhibited growth stop after induction with salicylate concentrations higher than 10 µM (Figure 1C). While this could be caused by metabolic burden, the fluorescence (and therefore the GFP amount) did not increase. High concentrations of salicylate decreased final OD_{600} in the other strains as well, but not as drastically (Figure 1D). This suggests that a feedback mechanism may be responsible for the growth inhibition. However, this behavior was not observed in previous experiments with the same promoter and may therefore be attributed to the expression of T7RNAP using a native promoter (Hanko et al., 2020). We decided not to pursue this strain further due to the potential impact of the native metabolism in future experiments. The rhamnose-inducible promoter yielded the highest *GFP* expression at 10 mM inducer concentration. However, the maximum fluorescence was comparable to that of the plasmid-based system. This is intriguing, since T7RNAP usually delivers higher protein levels due to the higher mRNA transcription rate (Studier and Moffatt, 1986). If the bottleneck lies in the translation phase, however, increasing the amount of mRNA would not influence the final protein yield. We speculated that this was the case in our *C. necator* T7R strain.

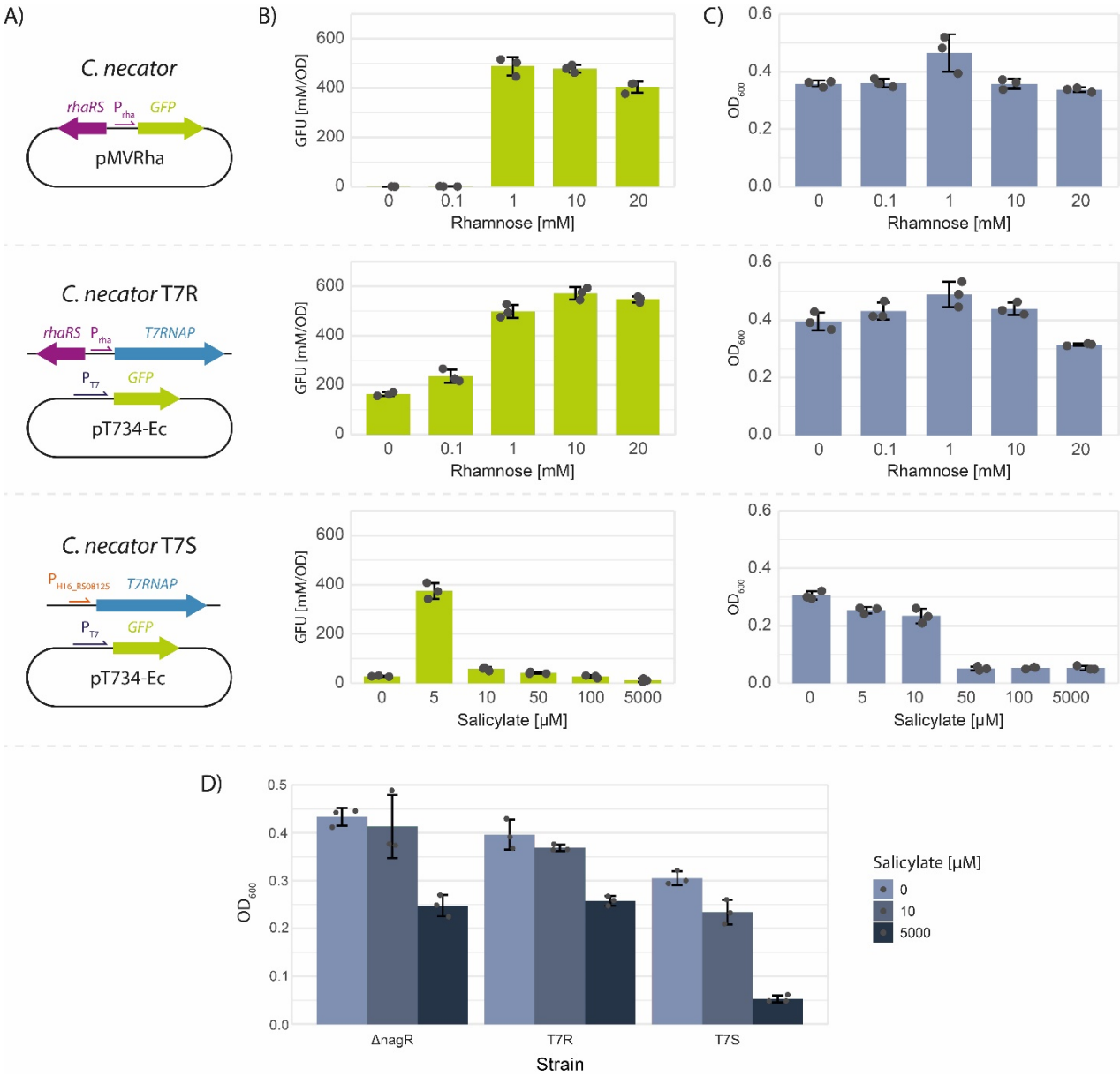

***Figure 1:* C. necator *strains containing genomically-integrated T7 RNA polymerase and producing GFP at different levels after induction with either rhamnose or salicylate as inducer**. *A) Genetic constructs introduced by genomic integration and plasmid transformation in the* C. necator *strains.* C. necator ΔnagR *carrying the pMVRha plasmid was used as a benchmark. B) Fluorescence values 22 hours after induction with different amounts of inducers, measured by plate reader. C) OD_{600} of different* C. necator *strains 22 hours after addition of different amounts of inducers, measured by plate reader. D) OD_{600} of different* C. necator *strains 22 hours after addition of different amounts of salicylate, measured by plate reader. For all figures, arithmetic means and standard deviations of three biological replicates are reported. Fluorescence is reported as GFU (Green Fluorescent Units: fluorescein equivalent units over OD_{600}).*

3.2 CODON USAGE IS THE LIMITING FACTOR FOR HIGH-YIELD PROTEIN PRODUCTION IN *CUPRIAVIDUS NECATOR*

We speculated that protein translation was limited by low ribosome occupancy (low RBS strength), or depletion of the cytoplasmic pool of charged tRNAs (non-optimal codon usage). We assembled multiple genetic constructs to investigate which variable was the bottleneck. Four plasmids were assembled, expressing *GFP* under the control of two RBSs (B0034m: 34; RBS A: A) (Figure 2A; Figure 5C). Two different *GFPmut3* genetic sequences were cloned, one from the original GoldenStandard library (Ec) and one codon-optimized for *C. necator* (Cn). All plasmids were introduced into *C. necator* T7R and analyzed for GFP production (Figure 2B). We could observe a striking increase in fluorescence (4-fold) when the codon-optimized gene was used, showing that codon usage (and tRNA pool depletion) was the process bottleneck. Even when using the pMVRha expression plasmid, codon optimization led to 2-fold increase in final fluorescence. On the other hand, increasing the strength of the RBS only slightly increased final fluorescence when using a suboptimal amount of inducer. Stronger RBSs also increased uninduced *GFP* expression, leading to higher leakiness.

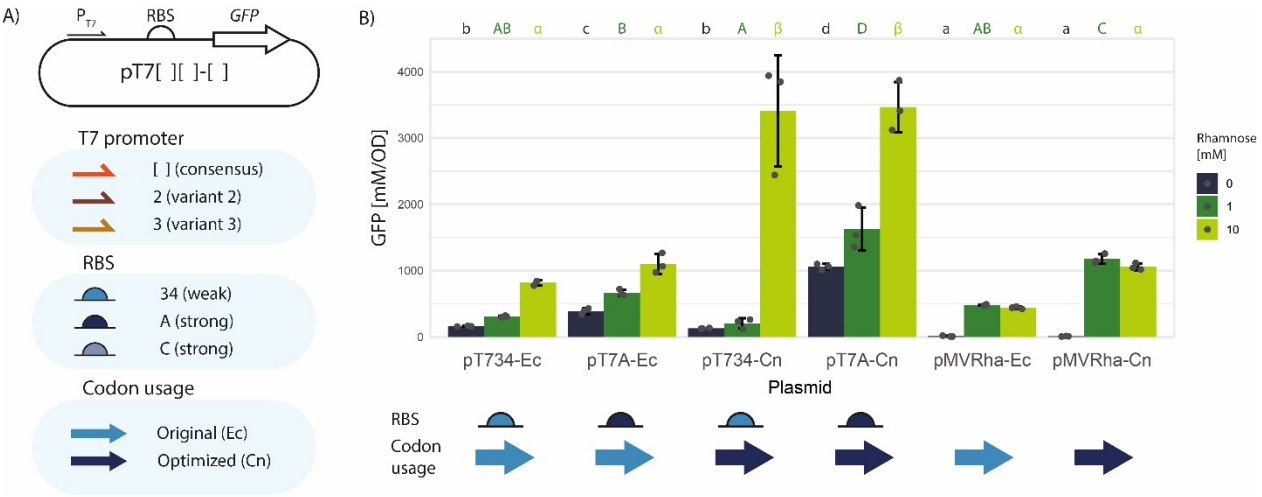

Figure 2: Genetic sequences are expressed at low level in* C. necator *when not codon optimized. *A) Genetic parts analyzed in this study. B) Fluorescence values after 22 hours of strain* C. necator *T7R expressing different* GFP *genetic sequences under the control of different RBS. For all figures, arithmetic means and standard deviations of three biological replicates are reported. Fluorescence is reported as GFU (Green Fluorescent Units: fluorescein equivalent units over* OD_{600}*).*

3.3 *CUPRIAVIDUS NECATOR* CONTAINS MORE RARE CODONS COMPARED TO *ESCHERICHIA COLI*

When we designed a codon-optimized *GFPmut3* sequence for *C. necator*, we found that the CAI for *E. coli* remained high (Figure 3A) (Sharp and Li, 1987). Thus, sequences that were optimal for *C. necator* were also optimal for *E. coli*, but not vice versa. This discrepancy could be traced to the codon usage of both organisms. We observed that the ratio of synonymous codons for each amino acid was balanced in *E. coli*. In contrast, it was common to encounter amino acids with imbalanced codon distributions in *C. necator*, with one codon prevalent and the others barely present in the genome. An example of this behaviour is shown in Figure 3B (the complete analysis can be found in Table S4). To quantify this phenomenon properly, we counted the number of codons at each frequency (Figure 3C). In *C. necator*, 23 codons were rare (used less than 10%), whereas in *E. coli*, this number decreased to six. This highlights the importance

of codon usage in *C. necator*, as previously reported (Mishra et al., 2024). The high number of rare codons suggests that many charged tRNAs may be present in lower quantities, potentially creating bottlenecks during protein production.

A)

	CAI (*C. necator*)	CAI (*E. coli*)	%GC	%GC3
GFP (Ec)	0.230	0.594	39.2	32.2
GFP (Cn)	0.662	0.674	56.5	81.6

B)

		Codon frequency [%]	
Amino acid	Codon	*C. necator*	*E. coli*
S	TCC	18	15
	TCA	4	12
	AGC	35	28
	TCT	3	15
	TCG	37	16
	AGT	3	14
V	GTG	59	37
	GTA	4	16
	GTC	32	21
	GTT	5	26

C)

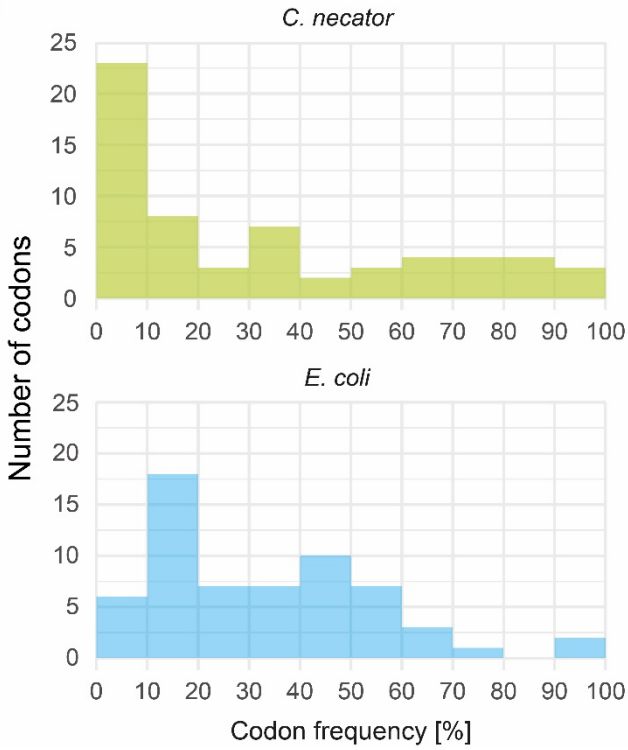

***Figure 3:* C. necator *contains a higher number of rare codons compared to* E. coli.** *A) Codon Adaptation Index (CAI) and GC percentage (both total - %GC; and of the third base of the codon - %GC3) of the two* GFPmut3 *genetic sequences in* E. coli *and* C. necator. *The original* GFP *sequence (*GFP *(Ec)) showed high CAI for E. coli, while the sequence optimized for* C. necator *(*GFP *(Cn)) showed high CAI for both organisms. B) Codon frequency of synonymous codons encoding serine and valine in both* E. coli *and* C. necator. *C) Number of codons present at each frequency in* C. necator *and* E. coli. C. necator *shows many codons with low and high frequencies, while in* E. coli *most codons are located in the intermediate range, showing a more balanced distribution.*

3.4 Newly designed T7 expression strains reduced leaky expression of the system

Although the maximum GFP production was satisfactory, the uninduced expression of the T7 system was higher than the one from pMVRha. Building on the knowledge gathered in our previous round of experiments, we thus proceeded to optimize the T7RNAP genetic construct. Our original system contained a non-codon-optimized T7RNAP sequence under the control of a strong RBS (RBS A). We hypothesized that codon-harmonizing the gene and selecting a weaker RBS would increase both maximum induction and tightness, and constructed a new strain with these modifications (*C. necator* T7R2, Figures 4A, S1). A new system for tightly regulating endonuclease expression in *C. necator* was recently established (Della Valle et al., 2025). Based on that work, we introduced a Self-splicing Intron-Based Riboswitch (SIBR) inside the T7RNAP coding sequence to increase tightness. The coding sequence was only complete when theophylline was added to the medium, due to SIBR self-catalysed excision. Accordingly, we planned two new strains: one with both induction systems (*C. necator* T7RT, Figures 4A, S1) and one with only SIBR, with the T7RNAP gene under the control of a strong constitutive promoter. Unfortunately, we could not

assemble the second strain and decided to abandon this strategy. The novel genetic circuits were integrated near the *nagR* locus. We chose not to delete *nagR*, since we initially suspected that our previous modification was responsible for the reduced rhamnose sensitivity observed in the *C. necator* T7R strain compared to pMVRha. However, this hypothesis proved to be incorrect (Figure S3). The reduced response is probably caused by lower copy number of the *rhaRS* responsive element. We induced *GFP* expression in *C. necator* T7RT with different concentrations of rhamnose and theophylline to identify the optimal conditions for this strain (Figure 4B). *GFP* expression proved tight, requiring high concentrations of both inducers to observe fluorescence production. This is consistent with the reported data from a similar system in *E. coli* (Della Valle et al., 2025). However, the maximum fluorescence obtained with strain *C. necator* T7RT was drastically lower than that obtained with the plasmid-based system. Conversely, strain *C. necator* T7R2 maintained the same maximum fluorescence as *C. necator* T7R while decreasing system leakiness by half (Figure 5C).

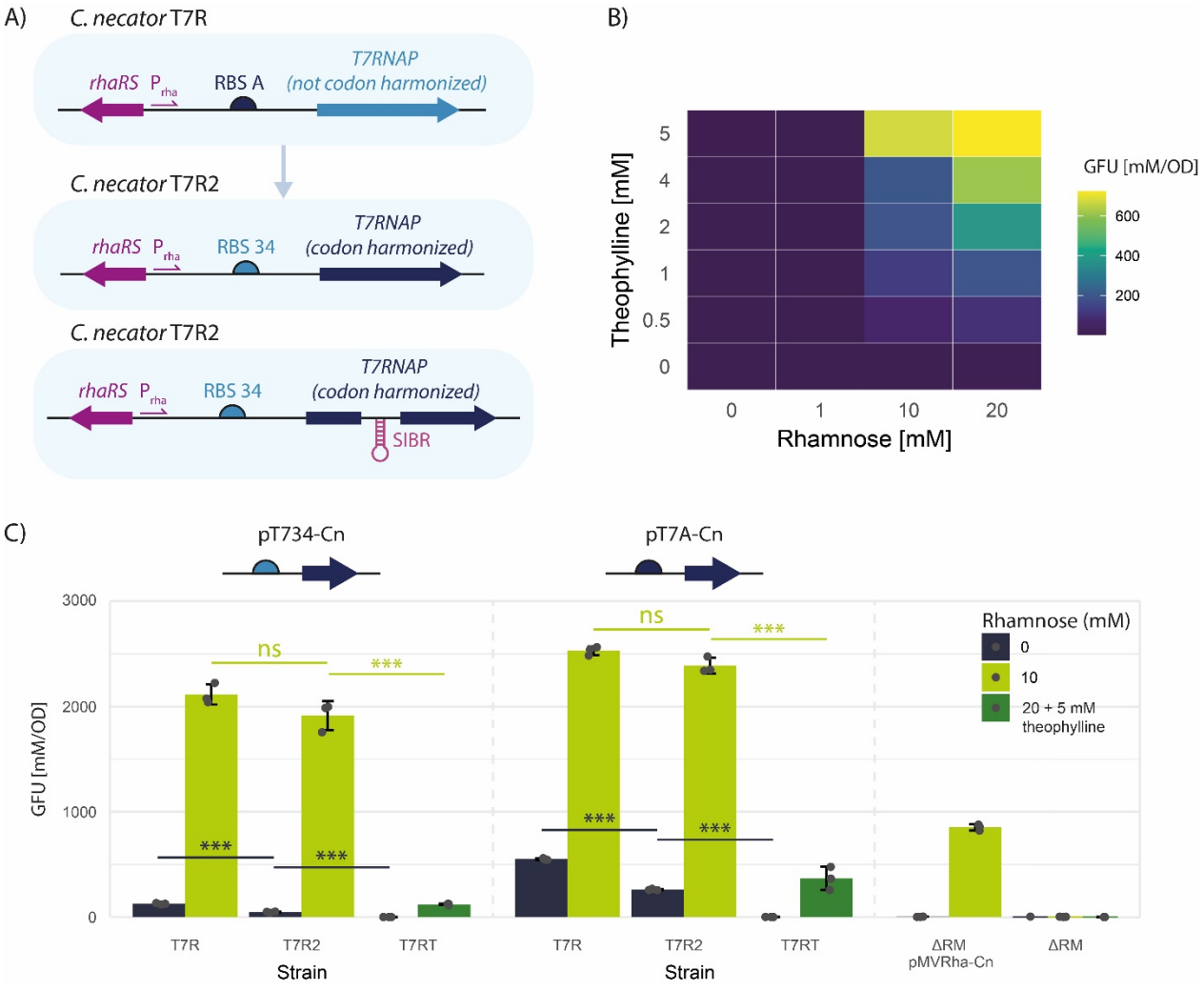

Figure 4: Strain* C. necator *T7R2 maintains maximum* GFP *expression and has lower leakiness compared to the parent strain. *A) Genetic constructs introduced by genomic integration in the new* C. necator *strains. B) Fluorescence expression values 22 hours after induction with different amounts of rhamnose and theophylline in strain* C. necator *T7RT carrying plasmid pT7A-Cn. C) Fluorescence values after 22 hours of different* C. necator *strains expressing* GFP *under the control of plasmids pT734-Cn and pT7A-Cn. For all figures, arithmetic means and standard deviations of three biological replicates are reported. Fluorescence is reported as GFU (Green Fluorescent Units: fluorescein equivalent units over* OD_{600}*).*

3.5 Optimization of genetic parts in the expression plasmid can further improve the system

After obtaining an optimized strain, we turned our attention to the expression plasmid. We assessed two new T7 promoter variants identified in previous studies for their higher performance compared to the consensus promoter (Conrad et al., 2020; Jones et al., 2015). We also designed a synthetic RBS derived from the highly efficient RBS present in the pET plasmid series, which has a slightly different Epsilon sequence that reflects the rRNA sequence in *C. necator* (RBS C) (Figure S2) (Olins and Rangwala, 1989). However, this RBS did not increase *GFP* expression compared to RBS A under the control of a constitutive promoter (Figure 5C). When applied in our T7 system, maximum fluorescence did not change drastically, while uninduced expression almost doubled (Figure 4B). These results confirmed our previous findings that increasing RBS strength increases leakiness. Increasing RBS strength from B0034m to RBS A increased both uninduced and induced expression. However, when we increased the RBS strength further, from RBS A to RBS C, only the uninduced expression increased significantly. This could indicate that another bottleneck in protein translation has been reached. Interestingly, both new T7 promoters were able to maintain the maximum protein expression; one variant also increased tightness (Figure 5A). Therefore, it was essential to optimize both the integrated genetic circuit and the plasmid-based expression system to achieve the desired effect. We introduced the best-performing plasmid (pT72A-Cn) into *E. coli* BL21(DE3) to compare the performance of our strain to the most widely used strain for bacterial protein production. When expressing *GFP* with this plasmid, our strain outperformed *E. coli* in terms of maximum expression and tightness (Figure 5D).

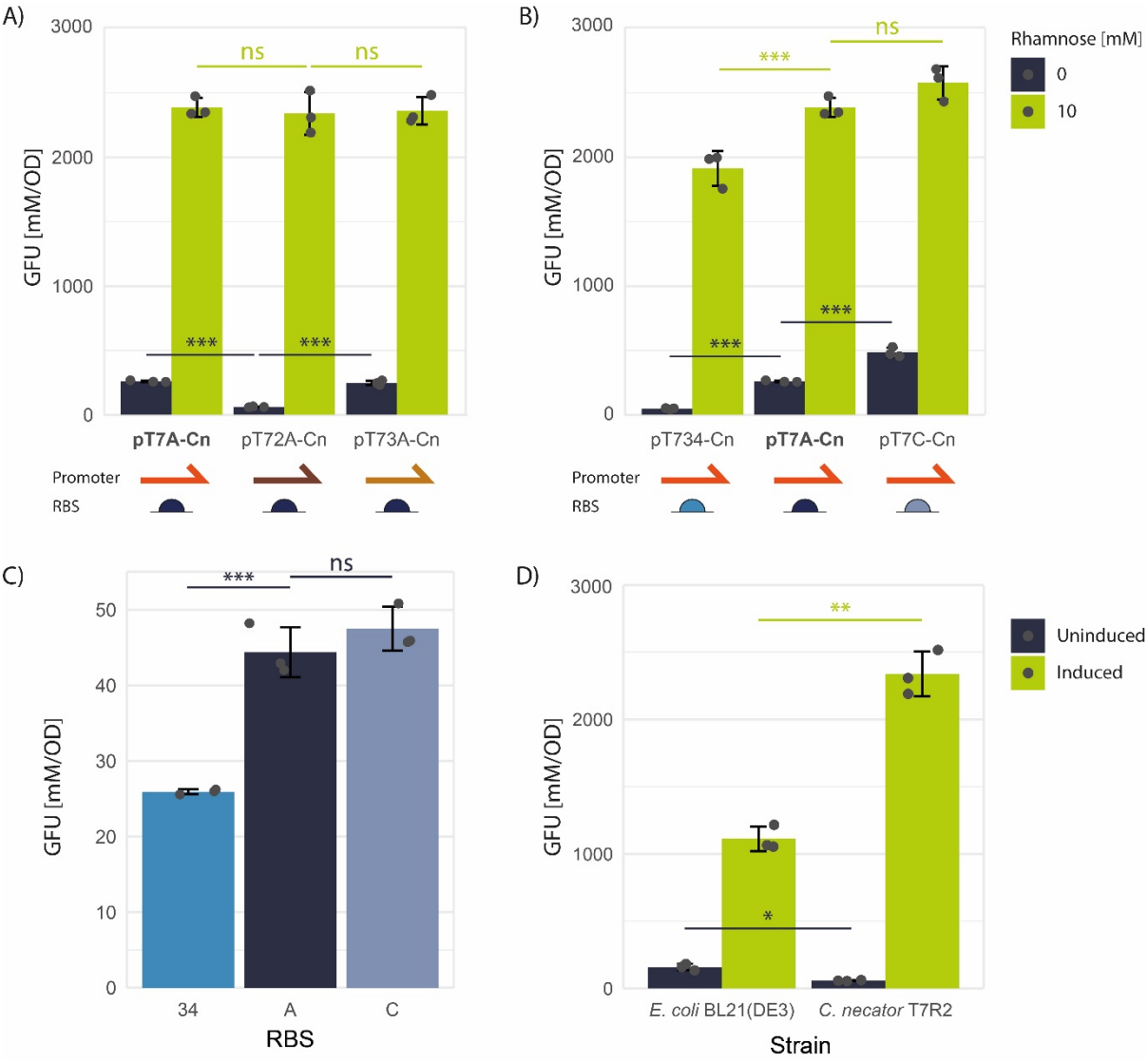

Figure 5: An optimized T7 promoter decreased leakiness while maintaining maximum fluorescence production. *A) Fluorescence values after 22 hours of strain* C. necator *T7R2 expressing* GFP *under the control of different T7 promoter variants. The best performing construct (as shown in Figure 4) is bold and used as reference. B) Fluorescence values after 22 hours of strain* C. necator *T7R2 expressing* GFP *under the control of different RBSs. The best performing construct (as shown in Figure 4) is bold and used as reference. C) Fluorescence expressed by constitutive promoter J23106 with the three different RBS analyzed in this study. D) Fluorescence values after 22 h of strains* C. necator *T7R2 and* E. coli *BL21(DE3) transformed with plasmid pT72A-Cn.* C. necator *was induced with 10 mM rhamnose,* E. coli *with 1 mM IPTG. Due to different autofluorescence in the two strains, measurements were blanked using a non-GFP producing strain. For all figures, arithmetic means and standard deviations of three biological replicates are reported. Fluorescence is reported as GFU (Green Fluorescent Units: fluorescein equivalent units over* OD_{600}*).*

3.6 ENE-REDUCTASE YQJM CAN BE EXPRESSED AT HIGH YIELD IN *C. NECATOR*

After optimizing *C. necator* for *GFP* expression, we used our highest-performing strain for enzyme production. We selected YqjM, a FMN-dependent ene-reductase from *Bacillus subtilis*, as a model enzyme due to its previous production in both *E. coli* (Pesic et al., 2017) and *C. necator* (Assil-Companioni et al., 2019; Vajente et al., 2025). We used our optimized system (*C. necator* T7R2, carrying plasmid pT72A with *C. necator* codon-harmonized *yqjM*) for the expression of YqjM, and to determine the most favourable culture conditions for producing this enzyme in *C. necator*. Thus, cultures were induced at different ODs

(0.4, 0.8, 1.2) and incubated at various temperatures after induction (22 °C, 26 °C, 30 °C). In addition, we used our plasmid-based expression system (pMVRha) to express both *E. coli* codon-optimized (Ec) and *C. necator* codon-harmonized (Cn) *yqjM* (Vajente et al., 2024) to confirm whether codon usage plays such an important role in enzyme expression. To compare our systems with a widely used expression strain, we produced the same protein in *E. coli* BL21(DE3) carrying the *E. coli* codon-optimized gene in plasmid pET28a. To determine the amount of active protein produced, we used a spectrophotometer-based quantification of the FMN cofactor produced in the soluble extract and calculated both specific FMN concentration (amount of FMN produced per OD unit) and total FMN concentration (amount of FMN produced by the whole culture). Wild-type strains were used as blanks, and we assumed that all the FMN produced by our cultures was bound to YqjM, yielding FMN-cofactor loaded protein. YqjM forms a tetramer in its active form, with one FMN molecule binding to each subunit (Kitzing et al., 2005). Surprisingly, the amount of FMN produced was higher in *C. necator* than in *E. coli* BL21(DE3) (Figure 6A). Thus, almost all growth conditions yielded a higher amount of active protein than the most commonly used protein expression strain *E. coli* BL21(DE3). Inducing at an earlier time point (OD_i 0.4) resulted in the highest FMN production per OD unit, but the final OD_{600} after 24 hours was lower compared to the other growth conditions (Figure S4B). Surprisingly, the highest amount of active enzyme (total FMN) was produced with our previously developed pMVRha plasmid carrying the codon-harmonized *yqjM* gene, as this culture reached a higher OD_{600} compared to the T7-based strain (Figure S4B). pMVRha expressing the codon-harmonized gene produced 3-fold more FMN-loaded enzyme compared to the non-harmonized one (Figure 6A), confirming the importance of codon usage tuning. According to our SDS-PAGE analysis, *E. coli* BL21(DE3) produced approximately twice as much soluble protein as our *C. necator* strains (Figure 6B). However, although *E. coli* produced more soluble enzyme, *C. necator* produced more FMN-loaded enzyme. Assuming one FMN molecule is equivalent to one YqjM subunit, the highest theoretical yield reached by *C. necator* was 106 mg/L of culture (Figure S4A). A thorough SDS-PAGE analysis quantification can be found in the Supplementary Information (Figure S5).

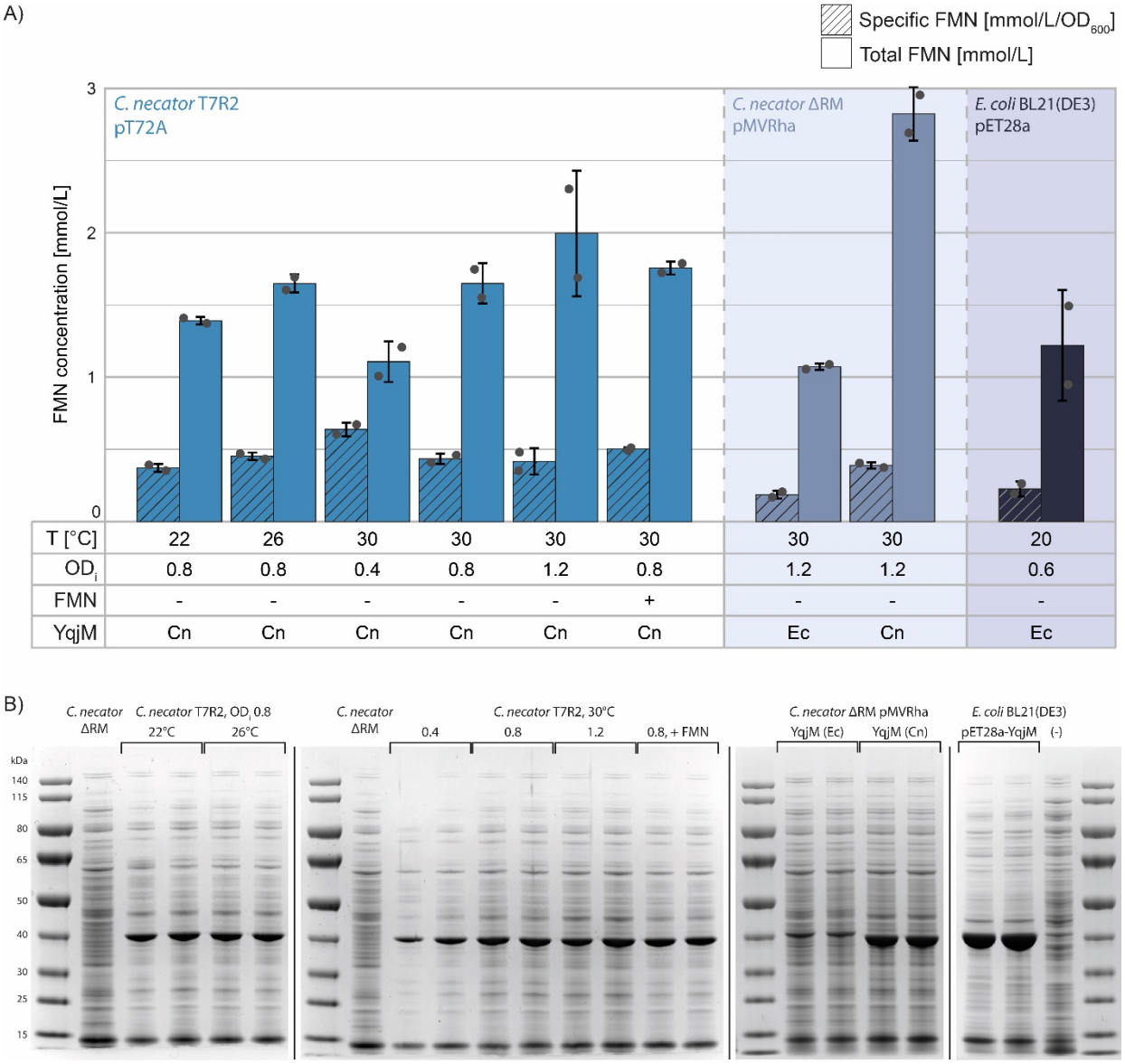

Figure 6:* C. necator *T7R2 shows the highest yield of FMN-bound soluble enzyme produced per OD_{600} of culture, but pMVRha produced the highest absolute amount of FMN-loaded enzyme. *A) FMN concentration in the soluble extract of* C. necator *T7R2 and other strains under different expression conditions. To calculate the specific FMN production, the total FMN quantity was divided by the final OD_{600} reached by each culture. FMN absorbance of each wild type strain without expression plasmid was used to blank the values. T[°C]: incubation temperature after induction; OD_i: induction OD; FMN: in one experiment (+), FMN was supplemented to the culture at a final concentration of 1 µM; YqjM: two sequences with different codon usages were used (Ec, Cn) (see Table S5 for CAI and Table S3 for sequences). Arithmetic means and standard deviations of two biological replicates are reported. FMN quantity is reported in mmol FMN/L of culture. B) SDS-PAGE analysis of the soluble extracts analyzed in Figure 6A. A gel-based normalized quantification of soluble protein production can be observed in the Supplementary Information (Figure S5).*

4 DISCUSSION

Given the high potential of *C. necator* for biocatalytic applications and C1-based manufacturing, there is an urgent need to develop more efficient protein production systems for this non-model host. In this study, we successfully integrated T7RNAP driven by two different inducible promoters. The native salicylate-based inducible promoter (NahR) was induced with micromolar amounts of inducer; however, higher amounts inhibited growth. Notably, this phenomenon has been observed not to be attributable to salicylate toxicity as previous studies have demonstrated that up to 5 mM of salicylate has been shown to be beneficial for growth (Hanko et al., 2020). In contrast, this was not the case in our study, even for the non-engineered strains. The difference in media composition may explain this discrepancy. The growth inhibition was unlikely due to the metabolic burden of T7RNAP or GFP production, as the cultures with impaired growth did not exhibit increased GFP fluorescence (Figure 1). Another previous attempt to use a heterologous salicylate promoter in *C. necator* achieved no protein production, further demonstrating that different genetic systems may interact differently with the native metabolism (Mishra et al., 2024). Since our goal was to develop a robust and reliable system, we decided to abandon the salicylate promoter and focus on the rhamnose-inducible strain. Although cell growth was maintained at all inducer concentrations, the maximum fluorescence obtained was comparable to that of our plasmid pMVRha. Previous attempts to establish a T7-based system in *C. necator* failed to overcome this challenge (Hu et al., 2020). We speculated that the high level of mRNA produced by the T7RNAP was not successfully translated into protein, creating a bottleneck in protein production. Thus, we focused our investigation on two variables: RBS strength and codon usage of the gene of interest. Using a stronger RBS increased uninduced expression considerably in our system while only slightly increasing maximum GFP fluorescence (Figures 2 and 5). This trade-off was disadvantageous, because tightness of the promoter is an essential quality in a production strain. Typically, separating the biomass accumulation phase from the protein production phase reduces the metabolic burden during growth, increases plasmid retention and final biomass, and leads to a higher protein yield. The main bottleneck in protein production was caused by the codon usage of the gene of interest. Optimizing the sequence of *GFPmut3* increased the maximum fluorescence by 4-fold compared to the non-optimized gene (Figure 2). Interestingly, our plasmid control also benefited from codon optimization, with a 2-fold increase in fluorescence. This indicates that protein translation was already a bottleneck when using the pMVRha plasmid. Another recent study also observed the role of codon tuning in protein production in *C. necator* (Mishra et al., 2024), and we confirmed that this bottleneck is relevant to both GFP production (Figure 2) and enzyme expression (Figure 5). By simply harmonizing the codons in the YqjM genetic sequence, the production of active enzyme using the pMVRha plasmid increased by almost 3-fold (Figure 5). While the role of codon usage in heterologous protein production has proven elusive in *E. coli*, with different proteins benefiting from codon optimization, harmonization, or non-optimized sequences (Claassens et al., 2017), the importance of this variable has been emphasized repeatedly (Liu et al., 2021). We found that most amino acids in *C. necator* show a strong bias towards specific codons. Conversely, *E. coli*'s synonymous codons are distributed more evenly (Figure 3). Each rare codon (used less than 10%) can impede protein production, and *C. necator* has almost four times more rare codons than *E. coli* (Figure 3). Building on this knowledge, we developed two new T7 strains using a weaker RBS to drive expression of a codon-harmonized T7RNAP. These modifications were intended to reduce uninduced T7RNAP expression while potentially increasing maximum protein production. The first goal was achieved with a 50% reduction in uninduced GFP fluorescence (Figure 4). However, an attempt to increase tightness using a newly developed theophylline-responsive system

(SIBR2.0) (Della Valle et al., 2025) was unsuccessful because the system was tight but not responsive to induction. This was unexpected because T7RNAP only requires low expression to drive high-level mRNA transcription. To further optimize our expression plasmid, we identified a T7 promoter variant that reduced uninduced expression and generated a tighter system (Figure 4). Our in-depth investigation of the genetic elements involved in the system revealed the importance of each variable's role and identified the bottlenecks limiting the desired phenotype. Ultimately, we compared the performance of our strain with *E. coli* BL21(DE3). When expressing *GFP* using the same plasmid, our strain exhibited lower uninduced expression and maximum fluorescence. Using our newly developed system, we expressed the flavin-dependent ene-reductase YqjM from *Bacillus subtilis*, to measure the strain's performance towards the production of an enzyme interesting for biocatalytic applications (Pesic et al., 2017). Our best strain (*C. necator* T7R2 pT72A) achieved the highest production of FMN-bound enzyme per biomass unit (Figure 6, Figure S5), demonstrating the success of our strategy in increasing the intracellular amount of YqjM. However, T7-based expression led to a considerable decrease in cell growth compared to plasmid-driven expression (Figure S4B). When producing YqjM using the pMVRha plasmid, the final yield of YqjM was higher than that obtained with our T7-based strains due to the higher final OD_{600}. A similar result was previously observed in *E. coli*, where some plasmid-based expression strains reached higher protein titers than usual T7-based expression (Schuster and Reisch, 2022). Both the pMVRha and the T7-based strain produced more total FMN-bound enzyme than *E. coli* BL21(DE3). With our best *C. necator* strain, a theoretical yield of 106 mg/L of FMN-bound YqjM was achieved, compared to 46 mg/L in *E. coli*. Optimizing the media composition and feeding strategy may further increase the final protein production.

In conclusion, our study demonstrates that *C. necator* is a promising industrial chassis for protein production. The T7-based system developed herein resulted in higher FMN-bound YqjM production per unit of biomass, whereas our previously developed plasmid pMVRha resulted in higher total production due to higher cell density achieved at the end of the growth phase. These systems can be used to produce enzymes that are difficult to express in *E. coli* due to the formation of inclusion bodies (Srinivasan et al., 2002) or a lack of cofactor maturation chaperones (Ryu et al., 2024). Even when producing different enzymes, our system outperformed *E. coli* in expressing FMN-bound soluble enzyme, further highlighting the potential of *C. necator* for biocatalysis applications. Furthermore, these optimized expression systems could also be used for lithoautotrophic or formatotrophic enzyme production, ultimately leading to CO_2-driven enzyme synthesis.

Declaration of competing interests

The authors declare that they have no known competing financial interests or personal relationships that could have influenced the work reported in this paper.

Acknowledgements

We thank Riccardo Clerici, Franziska Meier and all the employees at Formo GmbH for support and discussions, in particular Andrea Annibal and Emma Bassini for their insightful observations and experimental help.

Author contributions: CRediT

Matteo Vajente (RUG) – Conceptualization, Investigation, Writing – original draft

Hendrik Ballerstendt (RWTH-Aachen) – Supervision, Writing – review & editing

Lars M. Blank (RWTH-Aachen) – Resources, Supervision, Writing – review & editing

Sandy Schmidt (RUG) – Conceptualization, Supervision, Resources, Writing – review & editing

Funding sources

This project has received funding from the European Union's Horizon 2020 research and innovation programme under the Marie Skłodowska Curie grant agreement No 955740 and the Netherlands Organization for Scientific Research (OCENW.XS23.3.002).

5 BIBLIOGRAPHY

Alagesan, S., Hanko, E.K.R., Malys, N., Ehsaan, M., Winzer, K., Minton, N.P., 2018. Functional Genetic Elements for Controlling Gene Expression in Cupriavidus necator H16. Appl Environ Microbiol 84. https://doi.org/10.1128/AEM.00878-18

Angenent, S.C., Schuttinga, J.H., Van Efferen, M.F.H., Kuizenga, B., Van Bree, B., Van Der Krieken, R.O., Verhoeven, T.J., Wijffels, R.H., 2022. Hydrogen Oxidizing Bacteria as Novel Protein Source for Human Consumption: An Overview. TOMICROJ 16, e187428582207270. https://doi.org/10.2174/18742858-v16-e2207270

Arhar, S., Rauter, T., Stolterfoht-Stock, H., Lambauer, V., Kratzer, R., Winkler, M., Karava, M., Kourist, R., Emmerstorfer-Augustin, A., 2024. CO2-based production of phytase from highly stable expression plasmids in Cupriavidus necator H16. Microb Cell Fact 23, 9. https://doi.org/10.1186/s12934-023-02280-2

Assil-Companioni, L., Schmidt, S., Heidinger, P., Schwab, H., Kourist, R., 2019. Hydrogen-Driven Cofactor Regeneration for Stereoselective Whole-Cell C=C Bond Reduction in *Cupriavidus necator*. ChemSusChem cssc.201900327. https://doi.org/10.1002/cssc.201900327

Barnard, G.C., Henderson, G.E., Srinivasan, S., Gerngross, T.U., 2004. High level recombinant protein expression in Ralstonia eutropha using T7 RNA polymerase based amplification. Protein Expression and Purification 38, 264–271. https://doi.org/10.1016/j.pep.2004.09.001

Bernal-Cabas, M., Kumar, K., Terpstra, O., Van Den Bogaard, S., Ammar, A.B., Mäkinen, S., Herwig, L., De Almeida, M., Tervasmäki, P., Blank, L.M., Alter, T.B., Billerbeck, S., 2025. Food production from air: gas precision fermentation with hydrogen-oxidising bacteria. Trends in Biotechnology S016777992500321X. https://doi.org/10.1016/j.tibtech.2025.08.003

Blázquez, B., Torres-Bacete, J., Leon, D.S., Kniewel, R., Martinez, I., Sordon, S., Wilczak, A., Salgado, S., Huszcza, E., Popłoński, J., Prieto, M.A., Nogales, J., 2022. Golden Standard: A complete standard, portable, and interoperative MoClo tool for model and non-model bacterial hosts (preprint). Synthetic Biology. https://doi.org/10.1101/2022.09.20.508659

Byrom, D., 1994. Copolymer production. US5364778A.

Choi, J.H., Keum, K.C., Lee, S.Y., 2006. Production of recombinant proteins by high cell density culture of Escherichia coli. Chemical Engineering Science 61, 876–885. https://doi.org/10.1016/j.ces.2005.03.031

Claassens, N.J., Siliakus, M.F., Spaans, S.K., Creutzburg, S.C.A., Nijsse, B., Schaap, P.J., Quax, T.E.F., van der Oost, J., 2017. Improving heterologous membrane protein production in Escherichia coli by combining transcriptional tuning and codon usage algorithms. PLoS ONE 12, e0184355. https://doi.org/10.1371/journal.pone.0184355

Conrad, T., Plumbom, I., Alcobendas, M., Vidal, R., Sauer, S., 2020. Maximizing transcription of nucleic acids with efficient T7 promoters. Commun Biol 3, 439. https://doi.org/10.1038/s42003-020-01167-x

Della Valle, S., Orsi, E., Creutzburg, S.C.A., Jansen, L.F.M., Pentari, E.-N., Beisel, C.L., Steel, H., Nikel, P.I., Staals, R.H.J., Claassens, N.J., Van Der Oost, J., Huang, W.E., Patinios, C., 2025. Streamlined and efficient

genome editing in Cupriavidus necator H16 using an optimised SIBR-Cas system. Trends in Biotechnology S0167779925000435. https://doi.org/10.1016/j.tibtech.2025.02.006

Ehsaan, M., Baker, J., Kovács, K., Malys, N., Minton, N.P., 2021. The pMTL70000 modular, plasmid vector series for strain engineering in Cupriavidus necator H16. Journal of Microbiological Methods 189, 106323. https://doi.org/10.1016/j.mimet.2021.106323

Engler, C., Kandzia, R., Marillonnet, S., 2008. A One Pot, One Step, Precision Cloning Method with High Throughput Capability. PLoS ONE 3, e3647. https://doi.org/10.1371/journal.pone.0003647

Gruber, S., Schwendenwein, D., Magomedova, Z., Thaler, E., Hagen, J., Schwab, H., Heidinger, P., 2016. Design of inducible expression vectors for improved protein production in Ralstonia eutropha H16 derived host strains. Journal of Biotechnology 235, 92–99. https://doi.org/10.1016/j.jbiotec.2016.04.026

Hallamaa, M., Meier, H.P.F., Vajente, M., Ghirardi, M., Deska, J., Schmidt, S., 2025. Rieske Oxygenase-Catalyzed Biotransformations in Recombinant *Cupriavidus necator* Fueled by Formate Oxidation. ChemBioChem e202500722. https://doi.org/10.1002/cbic.202500722

Hanko, E.K.R., Paiva, A.C., Jonczyk, M., Abbott, M., Minton, N.P., Malys, N., 2020. A genome-wide approach for identification and characterisation of metabolite-inducible systems. Nat Commun 11, 1213. https://doi.org/10.1038/s41467-020-14941-6

Hu, M., Xiong, B., Li, Z., Liu, L., Li, S., Zhang, C., Zhang, X., Bi, C., 2020. A novel gene expression system for Ralstonia eutropha based on the T7 promoter. BMC Microbiol 20, 121. https://doi.org/10.1186/s12866-020-01812-9

Inoue, H., Nojima, H., Okayama, H., 1990. High efficiency transformation of Escherichia coli with plasmids. Gene 96, 23–28. https://doi.org/10.1016/0378-1119(90)90336-P

Ismail, S., Giacinti, G., Raynaud, C.D., Alfenore, S., Guillouet, S.E., Gorret, N., 2025. Characterization of Single Cell Protein produced by Cupriavidus necator grown on various nitrogen and carbon sources. Journal of Biotechnology S0168165625002093. https://doi.org/10.1016/j.jbiotec.2025.08.007

Ismail, S., Giacinti, G., Raynaud, C.D., Cameleyre, X., Alfenore, S., Guillouet, S., Gorret, N., 2024. Impact of the environmental parameters on single cell protein production and composition by Cupriavidus necator. Journal of Biotechnology 388, 83–95. https://doi.org/10.1016/j.jbiotec.2024.04.009

Jahn, M., Crang, N., Janasch, M., Hober, A., Forsström, B., Kimler, K., Mattausch, A., Chen, Q., Asplund-Samuelsson, J., Hudson, E.P., 2021. Protein allocation and utilization in the versatile chemolithoautotroph Cupriavidus necator. eLife 10, e69019. https://doi.org/10.7554/eLife.69019

Jhong, H.-R. "Molly," Ma, S., Kenis, P.J., 2013. Electrochemical conversion of CO2 to useful chemicals: current status, remaining challenges, and future opportunities. Current Opinion in Chemical Engineering 2, 191–199. https://doi.org/10.1016/j.coche.2013.03.005

Jones, J.A., Vernacchio, V.R., Lachance, D.M., Lebovich, M., Fu, L., Shirke, A.N., Schultz, V.L., Cress, B., Linhardt, R.J., Koffas, M.A.G., 2015. ePathOptimize: A Combinatorial Approach for Transcriptional Balancing of Metabolic Pathways. Sci Rep 5, 11301. https://doi.org/10.1038/srep11301

Keating, K.W., Young, E.M., 2023. Systematic Part Transfer by Extending a Modular Toolkit to Diverse Bacteria. ACS Synth. Biol. 12, 2061–2072. https://doi.org/10.1021/acssynbio.3c00104

Kitzing, K., Fitzpatrick, T.B., Wilken, C., Sawa, J., Bourenkov, G.P., Macheroux, P., Clausen, T., 2005. The 1.3 Å Crystal Structure of the Flavoprotein YqjM Reveals a Novel Class of Old Yellow Enzymes. Journal of Biological Chemistry 280, 27904–27913. https://doi.org/10.1074/jbc.M502587200

Lenz, O., Friedrich, B., 1998. A novel multicomponent regulatory system mediates H_2 sensing in *Alcaligenes eutrophus*. Proc. Natl. Acad. Sci. U.S.A. 95, 12474–12479. https://doi.org/10.1073/pnas.95.21.12474

Liu, Y., Yang, Q., Zhao, F., 2021. Synonymous but Not Silent: The Codon Usage Code for Gene Expression and Protein Folding. Annu. Rev. Biochem. 90, 375–401. https://doi.org/10.1146/annurev-biochem-071320-112701

Mishra, S., Perkovich, P.M., Mitchell, W.P., Venkataraman, M., Pfleger, B.F., 2024. Expanding the synthetic biology toolbox of *Cupriavidus necator* for establishing fatty acid production. Journal of Industrial Microbiology and Biotechnology 51, kuae008. https://doi.org/10.1093/jimb/kuae008

Olins, P.O., Rangwala, S.H., 1989. A novel sequence element derived from bacteriophage T7 mRNA acts as an enhancer of translation of the lacZ gene in Escherichia coli. J Biol Chem 264, 16973–16976.

Orita, I., Iwazawa, R., Nakamura, S., Fukui, T., 2012. Identification of mutation points in Cupriavidus necator NCIMB 11599 and genetic reconstitution of glucose-utilization ability in wild strain H16 for polyhydroxyalkanoate production. Journal of Bioscience and Bioengineering 113, 63–69. https://doi.org/10.1016/j.jbiosc.2011.09.014

Pan, H., Wang, J., Wu, H., Li, Z., Lian, J., 2021. Synthetic biology toolkit for engineering Cupriviadus necator H16 as a platform for CO2 valorization. Biotechnol Biofuels 14, 212. https://doi.org/10.1186/s13068-021-02063-0

Pesic, M., Fernández-Fueyo, E., Hollmann, F., 2017. Characterization of the Old Yellow Enzyme Homolog from *Bacillus subtilis* (YqjM). ChemistrySelect 2, 3866–3871. https://doi.org/10.1002/slct.201700724

Rice, P., Longden, I., Bleasby, A., 2000. EMBOSS: The European Molecular Biology Open Software Suite. Trends in Genetics 16, 276–277. https://doi.org/10.1016/S0168-9525(00)02024-2

Rosano, G.L., Morales, E.S., Ceccarelli, E.A., 2019. New tools for recombinant protein production in *Escherichia coli* : A 5-year update. Protein Science 28, 1412–1422. https://doi.org/10.1002/pro.3668

Ryu, H., Nguyen, C.N.M., Kuk Lee, S., Park, S., 2024. Development of Cupriavidus necator H16 as a host for heterologous production of formate dehydrogenase I of Methylorubrum extorquens: Possibilities and limitations. Bioresource Technology 394, 130187. https://doi.org/10.1016/j.biortech.2023.130187

Schiffels, J., Pinkenburg, O., Schelden, M., Aboulnaga, E.-H.A.A., Baumann, M.E.M., Selmer, T., 2013. An Innovative Cloning Platform Enables Large-Scale Production and Maturation of an Oxygen-Tolerant [NiFe]-Hydrogenase from Cupriavidus necator in Escherichia coli. PLoS ONE 8, e68812. https://doi.org/10.1371/journal.pone.0068812

Schuster, L.A., Reisch, C.R., 2022. Plasmids for Controlled and Tunable High-Level Expression in E. coli. Appl Environ Microbiol 88, e00939-22. https://doi.org/10.1128/aem.00939-22

Sharp, P.M., Li, W.-H., 1987. The codon adaptation index-a measure of directional synonymous codon usage bias, and its potential applications. Nucl Acids Res 15, 1281–1295. https://doi.org/10.1093/nar/15.3.1281

Shiloach, J., Fass, R., 2005. Growing E. coli to high cell density—A historical perspective on method development. Biotechnology Advances 23, 345–357. https://doi.org/10.1016/j.biotechadv.2005.04.004

Srinivasan, S., Barnard, G.C., Gerngross, T.U., 2002. A Novel High-Cell-Density Protein Expression System Based on *Ralstonia eutropha*. Appl Environ Microbiol 68, 5925–5932. https://doi.org/10.1128/AEM.68.12.5925-5932.2002

Studier, F.W., Moffatt, B.A., 1986. Use of bacteriophage T7 RNA polymerase to direct selective high-level expression of cloned genes. Journal of Molecular Biology 189, 113–130. https://doi.org/10.1016/0022-2836(86)90385-2

Sydow, A., Pannek, A., Krieg, T., Huth, I., Guillouet, S.E., Holtmann, D., 2017. Expanding the genetic tool box for Cupriavidus necator by a stabilized L-rhamnose inducible plasmid system. Journal of Biotechnology 263, 1–10. https://doi.org/10.1016/j.jbiotec.2017.10.002

Tanaka, K., Ishizaki, A., Kanamaru, T., Kawano, T., 1995. Production of poly(D-3-hydroxybutyrate) from CO_2, H_2, and O_2 by high cell density autotrophic cultivation of *Alcaligenes eutrophus*. Biotech & Bioengineering 45, 268–275. https://doi.org/10.1002/bit.260450312

The Galaxy Community, Abueg, L.A.L., Afgan, E., Allart, O., Awan, A.H., Bacon, W.A., Baker, D., Bassetti, M., Batut, B., Bernt, M., Blankenberg, D., Bombarely, A., Bretaudeau, A., Bromhead, C.J., Burke, M.L., Capon, P.K., Čech, M., Chavero-Díez, M., Chilton, J.M., Collins, T.J., Coppens, F., Coraor, N., Cuccuru, G., Cumbo, F., Davis, J., De Geest, P.F., De Koning, W., Demko, M., DeSanto, A., Begines, J.M.D., Doyle, M.A., Droesbeke, B., Erxleben-Eggenhofer, A., Föll, M.C., Formenti, G., Fouilloux, A., Gangazhe, R., Genthon, T., Goecks, J., Beltran, A.N.G., Goonasekera, N.A., Goué, N., Griffin, T.J., Grüning, B.A., Guerler, A., Gundersen, S., Gustafsson, O.J.R., Hall, C., Harrop, T.W., Hecht, H., Heidari, A., Heisner, T., Heyl, F., Hiltemann, S., Hotz, H.-R., Hyde, C.J., Jagtap, P.D., Jakiela, J., Johnson, J.E., Joshi, J., Jossé, M., Jum'ah, K., Kalaš, M., Kamieniecka, K., Kayikcioglu, T., Konkol, M., Kostrykin, L., Kucher, N., Kumar, A., Kuntz, M., Lariviere, D., Lazarus, R., Bras, Y.L., Corguillé, G.L., Lee, J., Leo, S., Liborio, L., Libouban, R., Tabernero, D.L., Lopez-Delisle, L., Los, L.S., Mahmoud, A., Makunin, I., Marin, P., Mehta, S., Mok, W., Moreno, P.A., Morier-Genoud, F., Mosher, S., Müller, T., Nasr, E., Nekrutenko, A., Nelson, T.M., Oba, A.J., Ostrovsky, A., Polunina, P.V., Poterlowicz, K., Price, E.J., Price, G.R., Rasche, H., Raubenolt, B., Royaux, C., Sargent, L., Savage, M.T., Savchenko, V., Savchenko, D., Schatz, M.C., Seguineau, P., Serrano-Solano, B., Soranzo, N., Srikakulam, S.K., Suderman, K., Syme, A.E., Tangaro, M.A., Tedds, J.A., Tekman, M., Cheng (Mike) Thang, W., Thanki, A.S., Uhl, M., Van Den Beek, M., Varshney, D., Vessio, J., Videm, P., Von Kuster, G., Watson, G.R., Whitaker-Allen, N., Winter, U., Wolstencroft, M., Zambelli, F., Zierep, P., Zoabi, R., 2024. The Galaxy platform for accessible, reproducible, and collaborative data analyses: 2024 update. Nucleic Acids Research 52, W83–W94. https://doi.org/10.1093/nar/gkae410

Tripathi, N.K., Shrivastava, A., 2019. Recent Developments in Bioprocessing of Recombinant Proteins: Expression Hosts and Process Development. Front. Bioeng. Biotechnol. 7, 420. https://doi.org/10.3389/fbioe.2019.00420

Vajente, M., Clerici, R., Ballerstedt, H., Blank, L.M., Schmidt, S., 2024. Using *Cupriavidus necator* H16 to Provide a Roadmap for Increasing Electroporation Efficiency in Nonmodel Bacteria. ACS Synth. Biol. acssynbio.4c00380. https://doi.org/10.1021/acssynbio.4c00380

Vajente, M., Ghirardi, M., Schmidt, S., 2025. Enzyme expression in Cupriavidus necator H16 for whole-cell biocatalysis, in: Methods in Enzymology. Elsevier, p. S0076687925001211. https://doi.org/10.1016/bs.mie.2025.01.079

Optimization of a T7 RNA polymerase expression system for high yield protein production in *Cupriavidus necator* H16

Matteo Vajente[1], Hendrik Ballerstedt[2], Lars M. Blank[2], Sandy Schmidt[1]

[1] Department of Chemical and Pharmaceutical Biology, Groningen Research Institute of Pharmacy, University of Groningen, Antonius Deusinglaan 1, Groningen 9713AV, The Netherlands.

[2] Institute of Applied Microbiology (iAMB), Aachen Biology and Biotechnology (ABBt), RWTH Aachen University, Worringerweg 1, 52074 Aachen, Germany, WSS research centre “catalaix”.

*Correspondence: s.schmidt@rug.nl

Supplementary Information

Supplementary Tables

Table S1: Plasmids used in this study.

Plasmid	Genotype	Reference
pMVRha	pBBR1 *rep*, *ori*; *Km*^{r}; RP4 *parABCDE*; *rhaRS*; $p_{J5[C2]}$-*spisPink*; RP4 *oriT*	(Vajente et al., 2024)
pMVRha-GFPEc	pMVRha; p_{rha}-*GFPmut3* (Ec)	This study
pMVRha-GFPCn	pMVRha; p_{rha}-*GFPmut3* (Cn)	This study
pMVRha-YqjM	pMVRha; p_{rha}-*yqjM* (Ec)	This study
pMVRha-YqjM-CnH	pMVRha; p_{rha}-*yqjM* (Cn)	This study
pET28a-YqjM	pET28a (pUC *ori*; *Km*^{r}; *lacI*) *yqjM* (Ec)	
pSEVA23g19[g1]	pBBR1 *rep*, ori; *Km*^{r}; *lacZ*	(Blázquez et al., 2022)
B0034_BD	pUC *ori*; *Amp*^{r}; RBS B0034m	(Blázquez et al., 2022)
GFP_DG	pUC *ori*; *Amp*^{r}; *GFPmut3* (Ec)	(Blázquez et al., 2022)
GFP_CnO_DG	pUC *ori*; *Amp*^{r}; *GFPmut3* (Cn)	This study
J23106_AB	pUC *ori*; *Amp*^{r}; Promoter J23106	(Blázquez et al., 2022)
B1006_GI	pUC *ori*; *Amp*^{r}; Terminator B1006	(Blázquez et al., 2022)
p10634-Cn	pSEVA23g19[g1]; J23106-B0034m-*GFPmut3* (Cn)-B1006	This study
p106A-Cn	pSEVA23g19[g1]; J23106-RBS_A-*GFPmut3* (Cn)-B1006	This study
p106C-Cn	pSEVA23g19[g1]; J23106-RBS_C-*GFPmut3* (Cn)-B1006	This study
pT734-Ec	pSEVA23g19[g1]; T7 (consensus)-B0034m-*GFPmut3* (Ec)-tT7hyb	This study
pT7A-Ec	pSEVA23g19[g1]; T7 (consensus)-RBS_A-*GFPmut3* (Ec)-tT7hyb	This study
pT734-Cn	pSEVA23g19[g1]; T7 (consensus)-B0034m-*GFPmut3* (Cn)-tT7hyb	This study
pT7A-Cn	pSEVA23g19[g1]; T7 (consensus)-RBS_A-*GFPmut3* (Cn)-B1006	This study
pT7C-Cn	pSEVA23g19[g1]; T7 (consensus)-RBS_C-*GFPmut3* (Cn)-tT7hyb	This study
pT72A-Cn	pSEVA23g19[g1]; T7 (variant 2)-RBS_A-*GFPmut3* (Cn)-tT7hyb	This study
pT73A-Cn	pSEVA23g19[g1]; T7 (variant 3)-RBS_A-*GFPmut3* (Cn)-tT7hyb	This study
pT72A-YqjM	pSEVA23g19[g1]; T7 (variant 2)-RBS_A-*yqjM* (Cn)-tT7hyb	This study
pLO3Mt	*Km*^{r}; *sacB*; RP4 *oriT*; pUC *ori*; silent mutation in restriction enzyme recognition site	(Vajente et al., 2024), adapted from (Lenz and Friedrich, 1998)
pLONagR	pLO3Mt; 1 kb homology regions near *nagR* for *nagR* deletion	This study

pLOT7R	pLO3Mt; 1 kb homology regions near *nagR* for *nagR* deletion; *rhaRS,* P_{rha}-RBS_A-*T7RNAP* (not codon optimized)	This study
pLOT7S	pLO3Mt; 1 kb homology regions near *nagR* for *nagR* deletion; $P_{H16\_RS08125}$-*T7RNAP* (not codon optimized)	This study; $P_{H16\_RS08125}$ from (Hanko et al., 2020)
pLOT7R2	pLO3Mt; 1 kb homology regions near *nagR*, without *nagR* deletion; *rhaRS,* P_{rha}-B0034m-*T7RNAP* (codon harmonized)	This study
pLOT7RT	pLO3Mt; 1 kb homology regions near *nagR*, without *nagR* deletion; *rhaRS,* P_{rha}-B0034m-*T7RNAP* (codon harmonized) with SIBR insertion between G442 and L443	This study

Table S2: Acceptor plasmids, donor plasmids, DNA fragments and oligonucleotides used for assembly of each plasmid.

Plasmid	**Fragments**	**Restriction enzyme**
pMVRha-GFPEc	pMVRha (acceptor plasmid) + GFP_DG (donor plasmid)	BsaI-HFv2
pMVRha-GFPCn	pMVRha (acceptor plasmid) + GFP_CnO_DG (donor plasmid)	BsaI-HFv2
pMVRha-YqjM	pMVRha (acceptor plasmid) + YqjM (Ec) (PCR-amplified from pET28a-YqjM using primers YqjM_BsaI_fw / YqjM_BsaI_rev)	BsaI-HFv2
pMVRha-YqjM-CnH	pMVRha (acceptor plasmid); YqjM (Cn) (synthesized by Twist Bioscience)	BsaI-HFv2
GFP_CnO_DG	Level 0 donor plasmid (PCR-amplified from GFP_DG using primers FPdonor_back_fw / FPdonor_back_rev) + GFP (Cn) (synthesized by Twist Bioscience)	BbsI-HF
p10634-Cn	pSEVA23g19[g1] (acceptor plasmid) + J23106_AB (donor plasmid) + B0034_BD (donor plasmid) + GFP_CnO_DG (donor plasmid) + B1006_GI (donor plasmid)	BsaI-HFv2
p106A-Cn	pSEVA23g19[g1] (acceptor plasmid) + J23106_AB (donor plasmid) + RBS_A (annealed oligonucleotides) + GFP_CnO_DG (donor plasmid) + B1006_GI (donor plasmid)	BsaI-HFv2
p106C-Cn	pSEVA23g19[g1] (acceptor plasmid) + J23106_AB (donor plasmid) + RBS_C (annealed oligonucleotides) + GFP_CnO_DG (donor plasmid) + B1006_GI (donor plasmid)	BsaI-HFv2
pT734-Ec	pSEVA23g19[g1] (acceptor plasmid) + T7 (consensus) (annealed oligonucleotides) + B0034_BD (donor plasmid) + GFP_ DG (donor plasmid) + tT7hyb (annealed oligonucleotides)	BsaI-HFv2
pT7A-Ec	pSEVA23g19[g1] (acceptor plasmid) + T7 (consensus) (annealed oligonucleotides) + RBS_A (annealed	BsaI-HFv2

	oligonucleotides) + GFP_ DG (donor plasmid) + tT7hyb (annealed oligonucleotides)	
pT734-Cn	pSEVA23g19[g1] (acceptor plasmid) + T7 (consensus) (annealed oligonucleotides) + B0034_BD (donor plasmid) + GFP_CnO_DG (donor plasmid) + tT7hyb (annealed oligonucleotides)	BsaI-HFv2
pT7A-Cn	pSEVA23g19[g1] (acceptor plasmid) + T7 (consensus) (annealed oligonucleotides) + RBS_A (annealed oligonucleotides) + GFP_CnO_DG (donor plasmid) + tT7hyb (annealed oligonucleotides)	BsaI-HFv2
pT7C-Cn	pSEVA23g19[g1] (acceptor plasmid) + T7 (consensus) (annealed oligonucleotides) + RBS_C (annealed oligonucleotides) + GFP_CnO_DG (donor plasmid) + tT7hyb (annealed oligonucleotides)	BsaI-HFv2
pT72A-Cn	pSEVA23g19[g1] (acceptor plasmid) + T7 (v2) (annealed oligonucleotides) + RBS_A (annealed oligonucleotides) + GFP_CnO_DG (donor plasmid) + tT7hyb (annealed oligonucleotides)	BsaI-HFv2
pT73A-Cn	pSEVA23g19[g1] (acceptor plasmid) + T7 (v3) (annealed oligonucleotides) + RBS_A (annealed oligonucleotides) + GFP_CnO_DG (donor plasmid) + tT7hyb (annealed oligonucleotides)	BsaI-HFv2
pT72A-YqjM	pSEVA23g19[g1] (acceptor plasmid) + T7 (v2) (annealed oligonucleotides) + RBS_A (annealed oligonucleotides) + YqjM (Cn) (synthesized by Twist Bioscience) + tT7hyb (annealed oligonucleotides)	BsaI-HFv2
pLONagR	pLO3NagR (linear backbone PCR-amplified from pLOT7R using primers pLOT7R_DOWN_fw/ pLONagR_UP_rev)	BsaI-HFv2
pLOT7R	pLO3Mt (linear backbone PCR-amplified from pLO3Mt using primers pLOT7R_pLO_fw/ pLOT7R_pLO_rev) + upstream homology region (PCR-amplified from *C. necator* genomic DNA using primers pLOT7R_UP_fw/pLOT7R_UP_rev) + terminator BBa_B0011 (annealed oligonucleotides) + Rhamnose promoter (PCR-amplified from pMVRha using primers pLOT7R_ Rha_fw /pLOT7R_ Rha_rev) + T7 RNA polymerase (PCR-amplified from *E. coli* BL21(DE3) genomic DNA using primers pLOT7R_T7_fw/ pLOT7R_T7_rev) + Terminator BBa_B0014 (synthesized by Twist Bioscience) + downstream homology region (PCR-amplified from *C. necator* genomic DNA using primers pLOT7R_DOWN_fw/ pLOT7R_DOWN_rev)	BsaI-HFv2
pLOT7S	pLO3Mt (linear backbone PCR-amplified from pLO3Mt using primers pLOT7R_pLO_fw/ pLOT7R_pLO_rev) + upstream homology region (PCR-amplified from *C. necator* genomic DNA using primers pLOT7R_UP_fw/pLOT7S_UP_rev) + terminator BBa_B0011 (annealed oligonucleotides) + Bba_B0015+ $P_{H16\_RS08125}$ (synthesized by Twist Bioscience) + T7 RNA polymerase	BsaI-HFv2

	(PCR-amplified from *E. coli* BL21(DE3) genomic DNA using primers pLOT7S_T7_fw/pLOT7R_T7_rev) + Terminator BBa_B0014 (synthesized by Twist Bioscience) + downstream homology region (PCR-amplified from *C. necator* genomic DNA using primers pLOT7R_DOWN_fw/ pLOT7R_DOWN_rev)	
pLOT7R2	pLOT7R (linear backbone PCR-amplified from pLOT7R using primers pLOT7R_pLO_fw / T7v2R_back_rev) + B0034_BD (donor plasmid) + T7 RNA polymerase (Cn) + BBa_B0014 (synthesized by Twist Bioscience) + downstream homology region (PCR-amplified from *C. necator* genomic DNA using primers T7v2R_DOWN_fw/ T7v2R_DOWN_rev)	BsaI-HFv2
pLOT7RT	pLOT7R (linear backbone PCR-amplified from pLOT7R using primers pLOT7R_pLO_fw / T7v2R_back_rev) + B0034_BD (donor plasmid) + T7 RNA polymerase (Cn), 1st fragment (PCR-amplified from pLOT7R using primers T7v2R_T7_fw / T7v2T_1_rev) + SIBR (synthesized by Twist Bioscience) + T7 RNA polymerase (Cn), 2nd fragment + BBa_B0014 (PCR-amplified from pLOT7R using primers T7v2T_2_fw / T7v2R_T7_rev) + downstream homology region (PCR-amplified from *C. necator* genomic DNA using primers T7v2R_DOWN_fw/ T7v2R_DOWN_rev)	BsaI-HFv2

Table S3: List of all genetic parts and fragments synthesized and used in this study. Restriction enzyme recognition sites are **bold**, restriction enzyme cutting sites are underlined.

Genetic part	**Sequence**	**Reference**	**Source**
Promoter T7 (consensus)	AA**GGTCTC**TGGAGTAATACGACTCACTATA GGGGAATACTT**GAGACC**TT	(Jones et al., 2015)	Synthesized as annealed oligonucleotides
Promoter T7 (variant 2)	AA**GGTCTC**TGGAGTAATACGACTCACTATC AAGGAATACTT**GAGACC**TT	(Jones et al., 2015), C4 promoter	Synthesized as annealed oligonucleotides
Promoter T7 (variant 3)	AA**GGTCTC**TGGAGTAATACGACTCACTATA GGGATAATTACTT**GAGACC**TT	(Conrad et al., 2020)	Synthesized as annealed oligonucleotides
Promoter J23106		(Blázquez et al., 2022)	Golden Standard library
RBS B0034m	**GGTCTC**TTACTAGAGAAAGAGGAGAAATA CTAAATGT**GAGACC**	(Blázquez et al., 2022)	Golden Standard library

RBS A	AA**GGTCTC**TTACTAATGAACAATTCTTAAGA AGGAGATATACAAATGT**GAGACC**TT	(Sydow et al., 2017)	Synthesized as annealed oligonucleotides
RBS C	AA**GGTCTC**TTACTATAATTTTGTTTAACCAG AAGAAGGAGATATACAATGT**GAGACC**TT	This study	Synthesized as annealed oligonucleotides
CDS *GFPmut3* (Ec)	**GGTCTC**TAATGATGCGTAAAGGAGAAGAA CTTTTCACTGGAGTTGTCCCAATTCTTGTTG AATTAGATGGTGATGTTAATGGGCACAAAT TTTCTGTCAGTGGAGAGGGTGAAGGTGAT GCAACATACGGAAAACTTACCCTTAAATTTA TTTGCACTACTGGAAAACTACCTGTTCCATG GCCAACACTTGTCACTACTTTCGGTTATGGT GTTCAATGCTTTGCGAGATACCCAGATCAT ATGAAACAGCATGACTTTTTCAAGAGTGCC ATGCCCGAAGGTTATGTACAGGAAAGAACT ATATTTTTCAAAGATGACGGGAACTACAAG ACACGTGCTGAAGTCAAGTTTGAAGGTGAT ACCCTTGTTAATAGAATCGAGTTAAAAGGT ATTGATTTTAAAGAAGATGGAAACATTCTT GGACACAAATTGGAATACAACTATAACTCA CACAATGTATACATCATGGCAGACAAACAA AAGAATGGAATCAAAGTTAACTTCAAAATT AGACACAACATTGAAGATGGAAGCGTTCAA CTAGCAGACCATTATCAACAAAATACTCCA ATTGGCGATGGCCCTGTCCTTTTACCAGAC AACCATTACCTGTCCACACAATCTGCCCTTT CGAAAGATCCCAACGAAAAGAGAGATCAC ATGGTCCTTCTTGAGTTTGTAACAGCTGCTG GGATTACACATGGCATGGATGAACTATACA AATAAGCTTT**GAGACC**	(Blázquez et al., 2022)	Golden Standard library
CDS *GFPmut3* (Cn)	**GAAGAC**AACCCC**GGTCTC**AAATGTCGAAG GGCGAAGAGCTGTTCACCGGGGTGGTACC CATCCTGGTGGAACTGGACGGCGATGTGA ACGGCCATAAGTTCTCGGTGTCGGGCGAG GGCGAGGGCGACGCCACGTACGGCAAGCT GACGCTCAAGTTCATCTGCACCACGGGCAA GCTGCCCGTGCCATGGCCTACCTTGGTGAC GACCTTCGGCTATGGAGTGCAGTGTTTCGC CCGCTATCCGGACCACATGAAGCAACATGA CTTTTTCAAGTCGGCCATGCCGGAGGGCTA CGTCCAGGAGCGCACCATCTTTTTCAAGGA TGACGGGAATTACAAGACGCGAGCTGAAG TGAAGTTTGAAGGCGACACCCTGGTGAACC GGATAGAGCTGAAGGGCATCGACTTCAAG GAGGATGGCAACATCCTGGGTCACAAGCT	This study	Synthesized by Twist bioscience

	GGAGTACAACTATAATTCCCACAACGTCTA CATCATGGCCGACAAGCAGAAGAACGGCA TCAAGGTCAACTTCAAGATCCGTCACAATAT CGAGGACGGGTCCGTGCAGCTCGCGGACC ACTATCAACAGAACACGCCGATCGGCGACG GCCCGGTGCTCCTGCCCGATAATCACTACCT TTCCACCCAGTCCGCATTGAGCAAGGACCC TAACGAAAAGCGTGACCATATGGTCCTGCT CGAGTTCGTCACTGCGGCCGGCATTACTCA CGGCATGGACGAGCTGTACAAATGAGCTTA **GAGACC**TACC**GTCTTC**		
CDS *yqjM* (Ec)	AA**GGTCTC**TAATGGGCAGCAGCCATCATCA TCATCATCACAGCAGCGGCCTGGTGCCGCG CGGCAGCCATATGGCCAGAAAATTATTTAC ACCTATTACAATTAAAGATATGACGTTAAA AAACCGCATTGTCATGTCGCCAATGTGCAT GTATTCTTCTCATGAAAAGGACGGAAAATT AACACCGTTCCACATGGCACATTACATATCG CGCGCAATCGGCCAGGTCGGACTGATTATT GTAGAGGCGTCAGCGGTTAACCCTCAAGG ACGAATCACTGACCAAGACTTAGGCATTTG GAGCGACGAGCATATTGAAGGCTTTGCAAA ACTGACTGAGCAGGTCAAAGAACAAGGTTC AAAAATCGGCATTCAGCTTGCCCATGCCGG ACGTAAAGCTGAGCTTGAAGGAGATATCTT CGCTCCATCGGCGATTGCGTTTGACGAACA ATCAGCAACACCTGTAGAAATGTCAGCAGA AAAAGTAAAAGAAACGGTCCAGGAGTTCA AGCAAGCGGCTGCCCGCGCAAAAGAAGCC GGCTTTGATGTGATTGAAATTCATGCGGCG CACGGATATTTAATTCATGAATTTTTGTCTC CGCTTTCCAACCATCGAACAGATGAATATG GCGGCTCACCTGAAAACCGCTATCGTTTCTT GAGAGAGATCATTGATGAAGTCAAACAAG TATGGGACGGTCCTTTATTTGTCCGTGTATC TGCTTCTGACTACACTGATAAAGGCTTAGA CATTGCCGATCACATCGGTTTTGCAAAATG GATGAAGGAGCAGGGTGTTGACTTAATTG ACTGCAGCTCAGGCGCCCTTGTTCACGCAG ACATTAACGTATTCCCTGGCTATCAGGTCA GCTTCGCTGAGAAAATCCGTGAACAGGCG GACATGGCTACTGGTGCCGTCGGCATGATT ACAGACGGTTCAATGGCTGAAGAAATTCTG CAAAACGGACGTGCCGACCTCATCTTTATC GGCAGAGAGCTTTTGCGGGATCCATTTTTT GCAAGAACTGCTGCGAAACAGCTCAATACA GAGATTCCGGCCCCTGTTCAATACGAAAGA GGCTGGTAAGCTTT**GAGACC**TT	(Zhang et al., 2019)	Kindly provided by Prof. Frank Hollmann (PCR-amplified from pET28a-YqjM)

CDS *yqjM* (Cn)	AA**GGTCTC**TAATGCACCATCACCACCATCAC ATGGCGCGCAAGCTGTTCACCCCCATCACC ATCAAGGACATGACGCTGAAGAACCGCATC GTGATGTCCCCCATGTGCATGTACAGCAGC CACGAGAAAGATGGCAAGCTGACCCCGTTT CATATGGCCCACTATATTTCCCGCGCCATCG GCCAGGTGGGCCTGATCATCGTCGAAGCCT CGGCCGTGAACCCCCAGGGCCGGATCACG GATCAGGATCTGGGCATCTGGAGCGATGA ACACATCGAGGGCTTCGCCAAGCTGACGGA ACAGGTGAAGGAGCAGGGGTCGAAGATCG GCATCCAGCTGGCGCACGCGGGCCGCAAG GCGGAACTGGAGGGCGACATCTTTGCGCC CTCCGCCATCGCCTTCGATGAGCAGTCGGC CACCCCCGTCGAGATGTCGGCCGAGAAGG TCAAGGAAACGGTGCAGGAATTTAAACAG GCCGCGGCGCGCGCCAAGGAGGCGGGCTT CGACGTGATCGAGATCCACGCCGCCCATGG CTACCTGATCCACGAGTTCCTGAGCCCGCT GTCCAACCACCGGACCGACGAGTACGGCG GCTCGCCCGAGAACCGCTACCGCTTTCTGC GCGAAATCATCGACGAGGTGAAGCAGGTC TGGGATGGGCCCCTGTTCGTGCGCGTCAGC GCGAGCGATTATACGGACAAGGGCCTGGA TATCGCGGACCATATCGGGTTCGCCAAGTG GATGAAAGAACAGGGGGTGGATCTGATCG ATTGCAGCTCGGGCGCGCTGGTGCATGCCG ATATCAACGTCTTTCCCGGCTACCAGGTGA GCTTTGCGGAAAAGATCCGCGAGCAGGCC GATATGGCGACGGGGGCGGTGGGCATGAT CACCGATGGGTCGATGGCGGAGGAGATCC TGCAGAACGGCCGCGCGGATCTCATCTTCA TCGGCCGCGAACTGCTGCGGGACCCCTTCT TCGCCCGCACGGCGGCCAAGCAGCTCAACA CCGAAATCCCGGCGCCCGTGCAGTATGAGC GCGGCTGGTGAGCTTT**GAGACC**TT	This study	Synthesized by Twist bioscience
Terminator tT7hyb	AA**GGTCTC**TGCTTAAACAGATAGGCCCTCT TCGGAGGGCCTATCTGTTTTTTTTTCGCTT**G** **AGACC**TT	(Calvopina-Chavez et al., 2022), T7hyb1	Synthesized as annealed oligonucleotides
Terminator B1006_GI	**GGTCTC**TGCTTAAAAAAAAACCCCGCCCCT GACAGGGCGGGGTTTTTTTTCGCTT**GAGAC** **C**	(Blázquez et al., 2022)	Golden Standard library
Terminator BBa_B0011	AA**GGTCTC**AAGAGAATATAAAAAGCCAGAT TATTAATCCGGCTTTTTTATTATTTT**GAGAC** **C**TA	iGEM website	Synthesized as annealed oligonucleotides

Terminator BBa_B0014	GT**GGTCTC**GGTAATCACACTGGCTCACCTTC GGGTGGGCCTTTCTGCGTTTATATACTAGA GAGAGAATATAAAAAGCCAGATTATTAATC CGGCTTTTTTATTATTTGCGAT**GAGACC**AA	iGEM website	Synthesized by Twist bioscience
Terminator BBa_B0015 + $P_{H16\_RS08125}$	GC**GGTCTC**GACCAGGCATCAAATAAAACGA AAGGCTCAGTCGAAAGACTGGGCCTTTCGT TTTATCTGTTGTTTGTCGGTGAACGCTCTCT ACTAGAGTCACACTGGCTCACCTTCGGGTG GGCCTTTCTGCGTTTATAGGTGCCGTCTATT ATTGATTTTATGAATGTTCATTATAGCCAGA ATTCTATTGGTTAATTTTCCTCCGTGCACCA TGATCCTTCCCATACGAAGAGACATAGCCG GAGACAT**GAGACC**AA	iGEM website, (Hanko et al., 2020)	Synthesized by Twist bioscience
SIBR	AA**GGTCTC**AAGGTTAATTGAGGCCTGAGTA TAAGGTGACTTATACTTGTAATCTATCTAAA CGGGGAACCTCTCTAGTAGACAATCCCGTG CTAAATTGATACCAGCATCGTCTTGATGCCC TTGGCAGCATAAATGCCTAACGACTATCCCT TTGGGGAGTAGGGTCAAGTGACTCGAAAC GATAGACAACTTGCTTTAACAAGTTGGAGA TATAGTCTGCTCTGCATGGTGACATGCAGC TGGATATAATTCCGGGGTAAGATTAACGAC CTTATCTGAACATAATGCTGCTCACGA**GAG ACC**AA	(Della Valle et al., 2025)	Synthesized by Twist bioscience
T7 RNA polymerase (Ec)	AA**GGTCTC**ATACAATGAACACGATTAACAT CGCTAAGAACGACTTCTCTGACATCGAACT GGCTGCTATCCCGTTCAACACTCTGGCTGA CCATTACGGTGAGCGTTTAGCTCGCGAACA GTTGGCCCTTGAGCATGAGTCTTACGAGAT GGGTGAAGCACGCTTCCGCAAGATGTTTGA GCGTCAACTTAAAGCTGGTGAGGTTGCGG ATAACGCTGCCGCCAAGCCTCTCATCACTAC CCTACTCCCTAAGATGATTGCACGCATCAAC GACTGGTTTGAGGAAGTGAAAGCTAAGCG CGGCAAGCGCCCGACAGCCTTCCAGTTCCT GCAAGAAATCAAGCCGGAAGCCGTAGCGT ACATCACCATTAAGACCACTCTGGCTTGCCT AACCAGTGCTGACAATACAACCGTTCAGGC TGTAGCAAGCGCAATCGGTCGGGCCATTGA GGACGAGGCTCGCTTCGGTCGTATCCGTGA CCTTGAAGCTAAGCACTTCAAGAAAAACGT TGAGGAACAACTCAACAAGCGCGTAGGGC ACGTCTACAAGAAAGCATTTATGCAAGTTG TCGAGGCTGACATGCTCTCTAAGGGTCTAC TCGGTGGCGAGGCGTGGTCTTCGTGGCATA AGGAAGACTCTATTCATGTAGGAGTACGCT GCATCGAGATGCTCATTGAGTCAACCGGAA TGGTTAGCTTACACCGCCAAAATGCTGGCG	(Studier and Moffatt, 1986)	PCR-amplified from *E. coli* BL21(DE3) genomic DNA

	TAGTAGGTCAAGACTCTGAGACTATCGAAC TCGCACCTGAATACGCTGAGGCTATCGCAA CCCGTGCAGGTGCGCTGGCTGGCATCTCTC CGATGTTCCAACCTTGCGTAGTTCCTCCTAA GCCGTGGACTGGCATTACTGGTGGTGGCTA TTGGGCTAACGGTCGTCGTCCTCTGGCGCT GGTGCGTACTCACAGTAAGAAAGCACTGAT GCGCTACGAAGACGTTTACATGCCTGAGGT GTACAAAGCGATTAACATTGCGCAAAACAC CGCATGGAAAATCAACAAGAAAGTCCTAGC GGTCGCCAACGTAATCACCAAGTGGAAGCA TTGTCCGGTCGAGGACATCCCTGCGATTGA GCGTGAAGAACTCCCGATGAAACCGGAAG ACATCGACATGAATCCTGAGGCTCTCACCG CGTGGAAACGTGCTGCCGCTGCTGTGTACC GCAAGGACAAGGCTCGCAAGTCTCGCCGTA TCAGCCTTGAGTTCATGCTTGAGCAAGCCA ATAAGTTTGCTAACCATAAGGCCATCTGGT TCCCTTACAACATGGACTGGCGCGGTCGTG TTTACGCTGTGTCAATGTTCAACCCGCAAG GTAACGATATGACCAAAGGACTGCTTACGC TGGCGAAAGGTAAACCAATCGGTAAGGAA GGTTACTACTGGCTGAAAATCCACGGTGCA AACTGTGCGGGTGTCGATAAGGTTCCGTTC CCTGAGCGCATCAAGTTCATTGAGGAAAAC CACGAGAACATCATGGCTTGCGCTAAGTCT CCACTGGAGAACACTTGGTGGGCTGAGCA AGATTCTCCGTTCTGCTTCCTTGCGTTCTGC TTTGAGTACGCTGGGGTACAGCACCACGGC CTGAGCTATAACTGCTCCCTTCCGCTGGCGT TTGACGGGTCTTGCTCTGGCATCCAGCACTT CTCCGCGATGCTCCGAGATGAGGTAGGTG GTCGCGCGGTTAACTTGCTTCCTAGTGAAA CCGTTCAGGACATCTACGGGATTGTTGCTA AGAAAGTCAACGAGATTCTACAAGCAGAC GCAATCAATGGGACCGATAACGAAGTAGTT ACCGTGACCGATGAGAACACTGGTGAAATC TCTGAGAAAGTCAAGCTGGGCACTAAGGC ACTGGCTGGTCAATGGCTGGCTTACGGTGT TACTCGCAGTGTGACTAAGCGTTCAGTCAT GACGCTGGCTTACGGGTCCAAAGAGTTCG GCTTCCGTCAACAAGTGCTGGAAGATACCA TTCAGCCAGCTATTGATTCCGGCAAGGGTC TGATGTTCACTCAGCCGAATCAGGCTGCTG GATACATGGCTAAGCTGATTTGGGAATCTG TGAGCGTGACGGTGGTAGCTGCGGTTGAA GCAATGAACTGGCTTAAGTCTGCTGCTAAG CTGCTGGCTGCTGAGGTCAAAGATAAGAA		

	GACTGGAGAGATTCTTCGCAAGCGTTGCGC TGTGCATTGGGTAACTCCTGATGGTTTCCCT GTGTGGCAGGAATACAAGAAGCCTATTCAG ACGCGCTTGAACCTGATGTTCCTCGGTCAG TTCCGCTTACAGCCTACCATTAACACCAACA AAGATAGCGAGATTGATGCACACAAACAG GAGTCTGGTATCGCTCCTAACTTTGTACACA GCCAAGACGGTAGCCACCTTCGTAAGACTG TAGTGTGGGCACACGAGAAGTACGGAATC GAATCTTTTGCACTGATTCACGACTCCTTCG GTACCATTCCGGCTGACGCTGCGAACCTGT TCAAAGCAGTGCGCGAAACTATGGTTGACA CATATGAGTCTTGTGATGTACTGGCTGATTT CTACGACCAGTTCGCTGACCAGTTGCACGA GTCTCAATTGGACAAAATGCCAGCACTTCC GGCTAAAGGTAACTTGAACCTCCGTGACAT CTTAGAGTCGGACTTCGCGTTCGCGTAAT**G AGAC**CTT		
T7 RNA polymerase (Cn) + terminator BBa_B0014	AA**GGTCTC**AAATGAACACGATCAACATCGC CAAGAACGACTTCTCGGACATCGAACTGGC CGCCATCCCCTTCAACACCCTGGCCGACCAT TACGGCGAGCGCCTCGCCCGCGAACAGCTC GCACTGGAGCATGAGTCGTACGAGATGGG CGAAGCACGCTTCCGCAAGATGTTTGAGCG CCAGCTGAAAGCCGGCGAGGTGGCAGATA ACGCCGCAGCAAAGCCGCTCATCACCACCC TCCTCCCGAAGATGATCGCACGCATCAACG ACTGGTTTGAGGAAGTGAAAGCCAAGCGC GGGAAGCGCCCCACGGCATTCCAGTTCCTG CAGGAAATCAAGCCCGAAGCAGTGGCATA CATCACCATCAAGACCACCCTGGCCTGCCTC ACCTCCGCCGACAATACGACCGTGCAGGCC GTGGCATCCGCAATCGGCCGTGCAATCGAG GACGAGGCCCGCTTCGGCCGCATCCGCGAC CTGGAAGCCAAGCACTTCAAGAAAAACGTG GAGGAACAGCTCAACAAGCGCGTGGGGCA CGTCTACAAGAAAGCATTTATGCAGGTGGT CGAGGCCGACATGCTCTCGAAGGGCCTCCT CGGCGGGGAGGCATGGTCGTCATGGCATA AGGAAGACTCGATCCATGTGGGGGTGCGC TGCATCGAGATGCTCATCGAGTCCACCGGG ATGGTGTCCCTCCACCGCCAGAATGCCGGG GTGGTGGGCCAGGACTCGGAAACCATCGA ACTCGCACCGGAATACGCCGAGGCCATCGC AACCCGCGCAGGCGCACTGGCCGGGATCT CGCCCATGTTCCAGCCGTGCGTGGTGCCGC CGAAGCCCTGGACCGGGATCACCGGCGGC GGGTATTGGGCCAACGGCCGCCGCCCGCT	This study, iGEM website	Synthesized by Twist Bioscience

	GGCACTGGTGCGCACCCACTCCAAGAAAGC ACTGATGCGCTACGAAGACGTGTACATGCC GGAGGTGTACAAAGCAATCAACATCGCACA GAACACGGCATGGAAAATCAACAAGAAAG TCCTCGCAGTCGCAAACGTGATCACCAAGT GGAAGCATTGCCCCGTCGAGGACATCCCG GCAATCGAGCGCGAAGAACTCCCCATGAAA CCCGAAGACATCGACATGAATCCGGAGGCC CTCACCGCATGGAAACGCGCCGCAGCCGCC GTGTACCGCAAGGACAAGGCCCGCAAGTC GCGCCGCATCTCCCTGGAGTTCATGCTGGA GCAGGCAAATAAGTTTGCCAACCATAAGGC AATCTGGTTCCCGTACAACATGGACTGGCG CGGCCGCGTGTACGCCGTGTCCATGTTCAA CCCCCAGGGCAACGATATGACCAAAGGGCT GCTGACGCTGGCAAAAGGCAAACCCATCG GCAAGGAAGGCTACTACTGGCTGAAAATCC ACGGCGCAAACTGCGCAGGCGTCGATAAG GTGCCCTTCCCGGAGCGCATCAAGTTCATC GAGGAAAACCACGAGAACATCATGGCCTG CGCCAAGTCGCCCCTGGAGAACACCTGGTG GGCCGAGCAGGATTCGCCCTTCTGCTTCCT GGCATTCTGCTTTGAGTACGCCGGGGTGCA GCACCACGGGCTGTCCTATAACTGCTCCCT GCCCCTGGCATTTGACGGGTCGTGCTCGGG GATCCAGCACTTCTCCGCAATGCTCCGGGA TGAGGTGGGCGGCCGCGCAGTGAACCTCC TGCCGTCCGAAACCGTGCAGGACATCTACG GGATCGTGGCCAAGAAAGTCAACGAGATC CTCCAGGCAGACGCAATCAATGGGACCGAT AACGAAGTGGTGACCGTGACCGATGAGAA CACCGGCGAAATCTCGGAGAAAGTCAAGCT GGGGACCAAGGCACTGGCCGGCCAGTGGC TGGCCTACGGCGTGACCCGCTCCGTGACCA AGCGCTCCGTCATGACGCTGGCCTACGGGT CCAAAGAGTTCGGGTTCCGCCAGCAGGTGC TGGAAGATACCATCCAGCCCGCCATCGATT CCGGGAAGGGCCTGATGTTCACCCAGCCCA ATCAGGCCGCCGGGTACATGGCCAAGCTG ATCTGGGAATCGGTGTCCGTGACGGTGGT GGCCGCAGTGGAAGCAATGAACTGGCTGA AGTCGGCCGCCAAGCTGCTGGCCGCCGAG GTCAAAGATAAGAAGACCGGGGAGATCCT GCGCAAGCGCTGCGCCGTGCATTGGGTGA CCCCGGATGGCTTCCCGGTGTGGCAGGAAT ACAAGAAGCCGATCCAGACGCGCCTCAACC TGATGTTCCTCGGCCAGTTCCGCCTCCAGCC GACCATCAACACCAACAAAGATTCCGAGAT		

	CGATGCACACAAACAGGAGTCGGGCATCG CCCCGAACTTTGTGCACTCCCAGGACGGCT CCCACCTGCGCAAGACCGTGGTGTGGGCAC ACGAGAAGTACGGGATCGAATCGTTTGCAC TGATCCACGACTCCTTCGGCACCATCCCCGC CGACGCCGCAAACCTGTTCAAAGCAGTGCG CGAAACCATGGTGGACACGTATGAGTCGT GCGATGTGCTGGCCGATTTCTACGACCAGT TCGCCGACCAGCTCCACGAGTCGCAGCTCG ACAAAATGCCCGCACTGCCCGCCAAAGGCA ACCTCAACCTCCGCGACATCCTCGAGTCAG ACTTCGCATTCGCGTAATCACACTGGCTCAC CTTCGGGTGGGCCTTTCTGCGTTTATATACT AGAGAGAGAATATAAAAAGCCAGATTATTA ATCCGGCTTTTTTATTATTTGCGAATCCTCG TAGGTACCACTAT**GAGACC**TT		

Table S4: Codon usage tables of *E. coli* BL21 (NCBI: GCF_013166975) and *C. necator* H16 (NCBI: GCF_004798725) calculated using cusp (EMBOSS).

Codon	**AA**	**Frequency *E. coli* [%]**	**Frequency *C. necator* [%]**
GCA	A	21.3	8.9
GCC		26.8	47.4
GCG		35.6	39.1
GCT		16.2	4.6
TGC	C	55.4	90.5
TGT		44.6	9.5
GAC	D	37.3	73.8
GAT		62.7	26.2
GAA	E	69.3	40.2
GAG		30.7	59.8
TTC	F	42.7	81.5
TTT		57.3	18.5
GGA	G	10.8	4.6
GGC		40.4	75.3
GGG		15.0	12.6
GGT		33.8	7.5
CAC	H	43.3	63.9
CAT		56.7	36.1
ATA	I	7.4	1.9
ATC		41.9	86.1

ATT		50.8	12.0
AAA	K	76.6	10.3
AAG		23.4	89.7
CTA	L	3.6	1.2
CTC		10.5	13.8
CTG		49.7	74.0
CTT		10.3	4.8
TTA		13.0	0.3
TTG		12.8	5.9
ATG	M	100.0	100.0
AAC	N	55.0	76.2
AAT		45.0	23.8
CCA	P	19.1	5.9
CCC		12.3	27.4
CCG		52.7	60.8
CCT		15.8	5.9
CAA	Q	34.8	14.0
CAG		65.2	86.0
AGA	R	3.7	0.9
AGG		2.2	3.8
CGA		6.5	2.8
CGC		40.0	67.3
CGG		9.7	17.5
CGT		37.9	7.6
AGC	S	27.6	35.0
AGT		15.0	3.5
TCA		12.4	3.9
TCC		14.9	18.0
TCG		15.6	36.9
TCT		14.6	2.7
ACA	T	13.0	4.1
ACC		43.3	57.0
ACG		26.9	34.3
ACT		16.8	4.6
GTA	V	15.6	4.0
GTC		21.4	32.2
GTG		37.1	58.8
GTT		26.0	5.0
TGG	W	100.0	100.0
TAC	Y	42.9	69.8

TAT		57.1	30.2
TAA	*	61.7	16.7
TAG		7.7	16.0
TGA		30.6	67.3

Table S5: Table of calculated Codon Adaptation Index values (CAI) for all genes expressed in this study.

Gene	**CAI *E. coli* BL21 (NCBI: GCF_013166975)**	**CAI *C. necator* H16 (NCBI: GCF_004798725)**
GFPmut3 (Ec)	0.594	0.230
GFPmut3 (Cn)	0.674	0.662
T7 RNA polymerase (Ec)	0.656	0.380
T7 RNA polymerase (Cn)	0.715	0.697
yqjM (Ec)	0.665	0.304
yqjM (Cn)	0.757	0.789

Table S6: List of primers used in this study.

Name	**Sequence**
RBS_A_fw	AAGGTCTCATACTAATGAACAATTCTTAAGAAGGAGATATACAAATGAGAGACCAA
RBS_A_rev	TTGGTCTCTCATTTGTATATCTCCTTCTTAAGAATTGTTCATTAGTATGAGACCTT
RBS_C_fw	AAGGTCTCATACTATAATTTTGTTTAACCAGAAGAAGGAGATATACAATGAGAGACCAA
RBS_C_rev	TTGGTCTCTCATTGTATATCTCCTTCTTCTGGTTAAACAAAATTATAGTATGAGACCTT
T7p_fw	GGGTCTCAGGAGTAATACGACTCACTATAGGGGAATACTAGAGACCG
T7p_rev	CGGTCTCTAGTATTCCCCTATAGTGAGTCGTATTACTCCTGAGACCC
T7t_fw	GGGTCTCAGCTTAAACAGATAGGCCCTCTTCGGAGGGCCTATCTGTTTTTTTTTCGCTAGAGACCG
T7t_rev	CGGTCTCTAGCGAAAAAAAAACAGATAGGCCCTCCGAAGAGGGCCTATCTGTTTAAGCTGAGACCC
pLOT7R_pLO_fw	AAGGTCTCACTGCAGGCATGCAAGCTAATTCTC
pLOT7R_pLO_rev	AAGGTCTCACCCCGGGTACCGAGCTCG
pLOT7R_UP_fw	AAGGTCTCAGGGGTGACGCGCCGCGTCGCAGG
pLOT7R_UP_rev	AAGGTCTCACTCTCTACGAGCTGAAGCAGTAGTGCC
pLOT7S_UP_rev	AAGGTCTCATGGTCTACGAGCTGAAGCAGTAGTGCC
pLOT7R_Rha_fw	AAGGTCTCAATTTTTAATCTTTCTGCGAATTGAG
pLOT7R_Rha_rev	AAGGTCTCATGTATATCTCCTTCTTAAGAATTG
pLOT7R_T7_fw	AAGGTCTCATACAATGAACACGATTAACATCGC
pLOT7R_T7_rev	AAGGTCTCATTACGCGAACGCGAAGTC
pLOT7S_T7_fw	AAGGTCTCAGACAATGAACACGATTAACATCGC
pLOT7R_DOWN_fw	AAGGTCTCAGCGAATCCTCGTAGGTACCAGAG

pLOT7R_DOWN_rev	AAGGTCTCAGCAGGCTGCGCTCGCGTGGTCTTC
pLONagR_UP_rev	AAGGTCTCATCGCCTACGAGCTGAAGCAGTAGTGCC
T7v2R_back_rev	AAGGTCTCAAGTATACGACCAGTCTAAAAAGCGCC
T7v2R_T7_fw	AAGGTCTCAAATGAACACGATCAACATCG
T7v2R_T7_rev	AAGGTCTCATAGTGGTACCTACGAGGATTCGC
T7v2R_DOWN_fw	AAGGTCTCAACTACTGCTTCAGCTCGTAGAAATC
T7v2R_DOWN_rev	AAGGTCTCAGCAGGCCTTAATCACCATAACCCACG
T7v2T_1_rev	AAGGTCTCAACCTTTGGTCATATCGTTGC
T7v2T_2_fw	AAGGTCTCACACGCTGGCAAAAGGCAAAC
FPdonor_back_fw	AGAAGACAACCTAGGGTACCGAGCTCGAATTCA
FPdonor_back_rev	AGAAGACAAGGGGATCCTCTAGAGTCGAC
YqjM_BsaI_fw	AAGGTCTCTAATGGGCAGCAGCCATCATC
YqjM_BsaI_rev	AAGGTCTCAAAGCTTACCAGCCTCTTTCGTATTGAA

Supplementary Figures

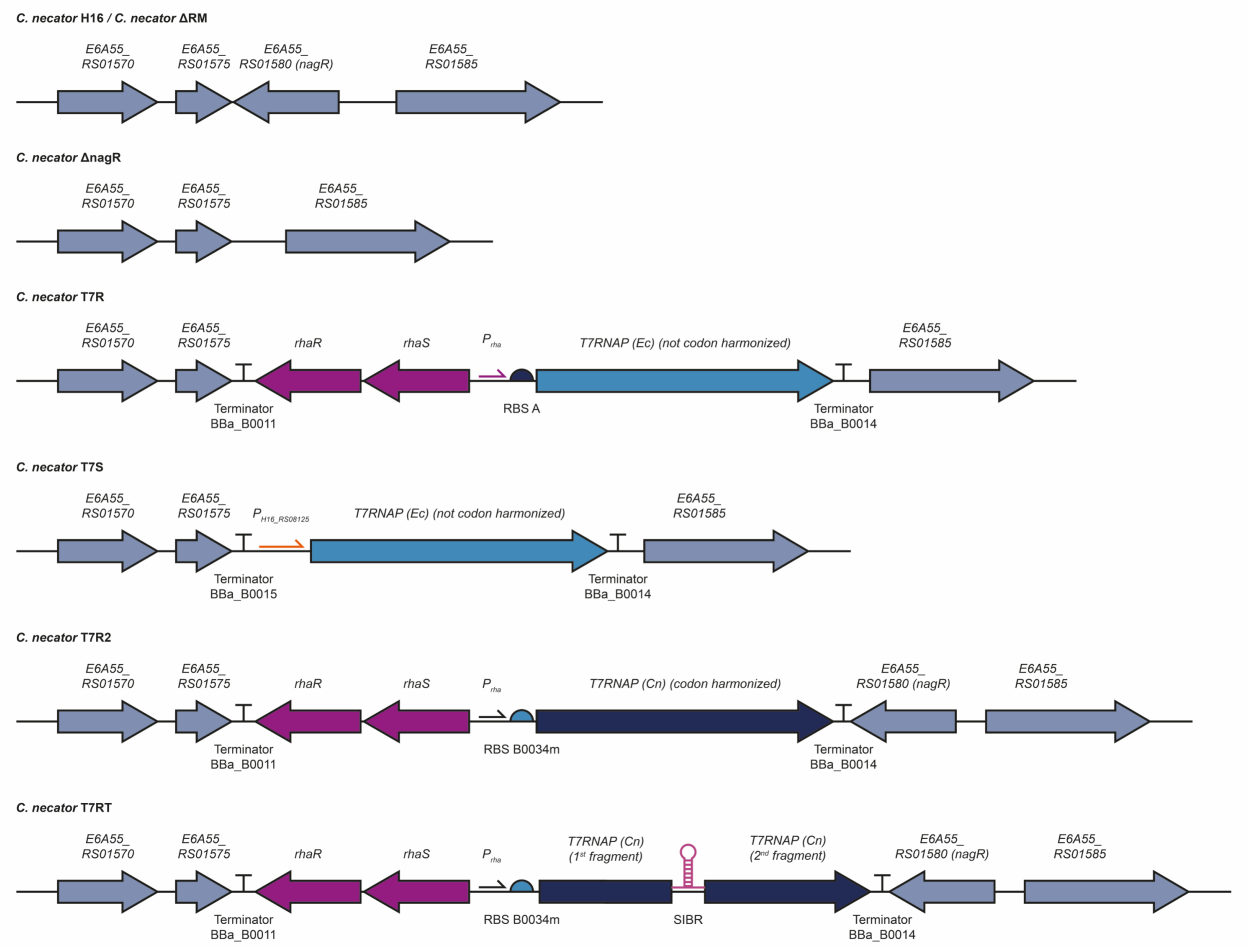

Figure S1: Schematic representation of the genotype of all strains created in this manuscript.

Figure S2: Design of RBS C for *C. necator*. A) Zoom-in of the alignment between rRNA sequences of E. coli and C. necator, with the original Epsilon sequence highlighted. B) Alignment of the pET RBS sequence (T7RBS from the Golden Standard library) and the newly designed RBS C.

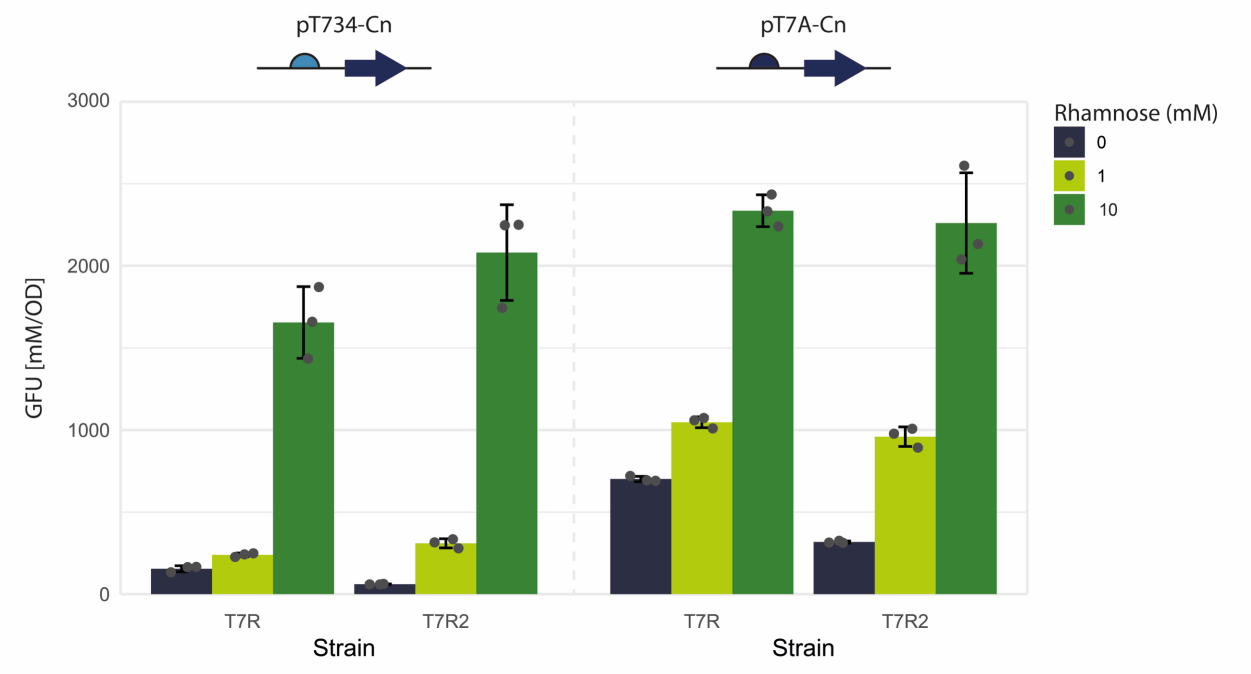

Figure S3: *C. necator* T7R and *C. necator* T7R2 have the same response to different concentrations of rhamnose. Fluorescence values after 22 hours of different *C. necator* strains expressing *GFP* under the control of plasmids pT734-Cn and pT7A-Cn. For all figures, arithmetic means and standard deviations of three biological replicates are reported. Fluorescence is reported as GFU (Green Fluorescent Units: fluorescein equivalent units over OD_{600}).

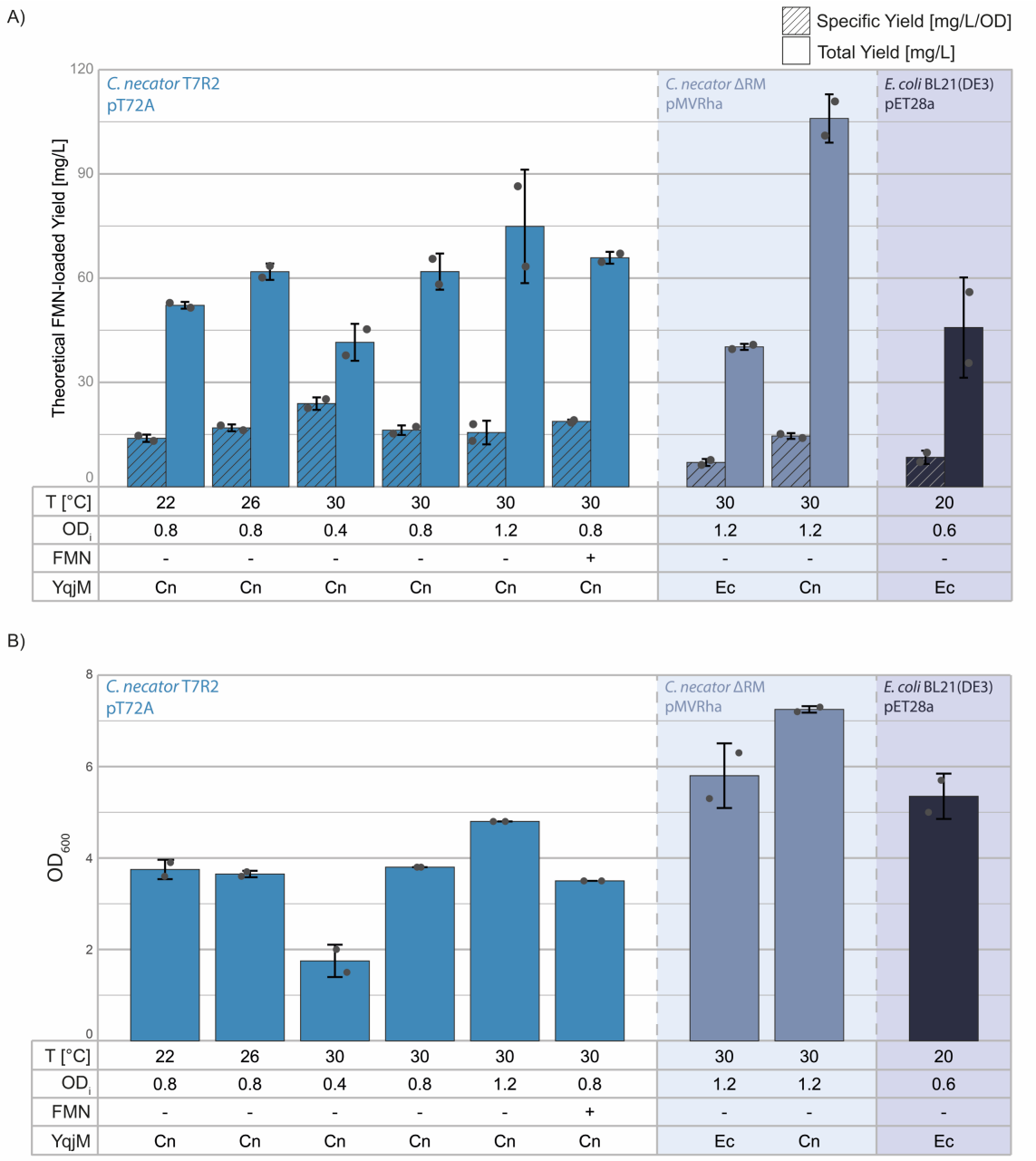

Figure S4: Theoretical yield of FMN-loaded enzyme and OD_{600} reached by the strains analyzed in Figure 6. A) Theoretical yield of FMN-loaded enzyme produced by the strains analyzed in Figure 6. The calculations were performed assuming that one molecule of FMN is equal to one protein. B) OD_{600} reached by the strains at the moment of harvest, measured by a spectrophotometer. T[°C]: incubation temperature after induction; OD_i: induction OD_{600}; FMN: in one experiment (+), FMN was supplemented to the culture at a final concentration of 1 µM; YqjM: two sequences with different codon usages were used (Ec, Cn) (see Table S5 for CAI and Table S3 for sequences). Arithmetic means and standard deviations of two biological replicates are reported.

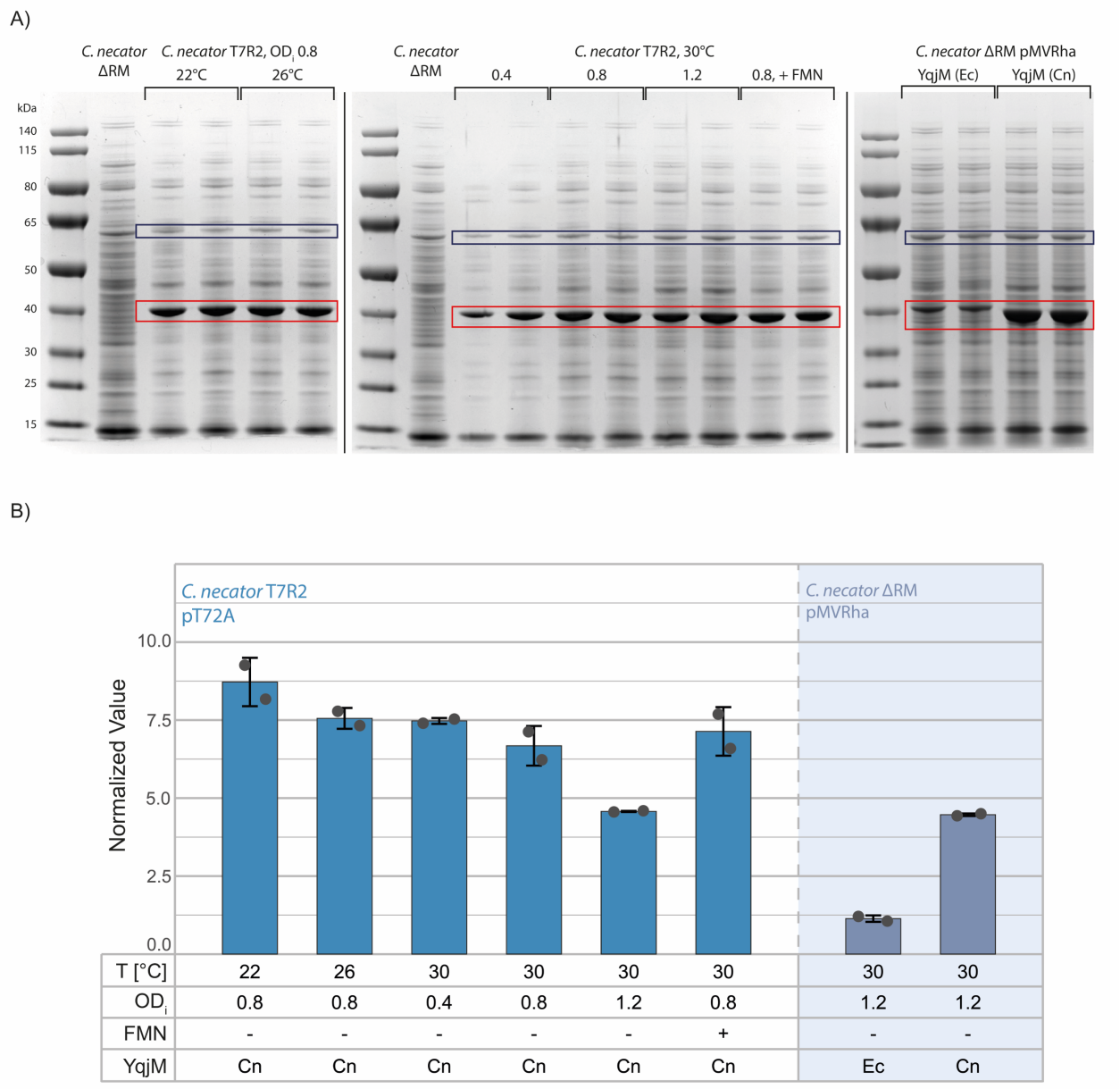

Figure S5: **Relative quantification of soluble YqjM produced by *C. necator* in different conditions, measured from SDS-PAGE.** The YqjM band intensity (red square) was divided by another protein band's intensity (blue square) in order to normalize the data. The assumption is that the intensity of this second band is constants in all conditions tested. Band intensities were quantified using the Gel Analysis tools from Fiji (Schindelin et al., 2012). T[°C]: incubation temperature after induction; OD_i: induction OD_{600}; FMN: in one experiment (+), FMN was supplemented to the culture at a final concentration of 1 µM; YqjM: two sequences with different codon usages were used (Ec, Cn) (see Table S5 for CAI and Table S3 for sequences). Arithmetic means and standard deviations of two biological replicates are reported.